NACA RM E56A19

NACA

RESEARCH MEMORANDUM

A STUDY OF FUEL-NITRIC ACID REACTIVITY

By Charles E. Feiler and Louis Baker, Jr.

Lewis Flight Propulsion Laboratory
Cleveland, Ohio

NATIONAL ADVISORY COMMITTEE
FOR AERONAUTICS
WASHINGTON

April 6, 1956
Declassified February 26, 1958

NATIONAL ADVISORY COMMITTEE FOR AERONAUTICS

RESEARCH MEMORANDUM

A STUDY OF FUEL-NITRIC ACID REACTIVITY

By Charles E. Feiler and Louis Baker, Jr.

SUMMARY

The relative reactivities of six fuels with red fuming nitric acid (19 percent NO_2) were determined in a 40-pound-thrust rocket engine with rapid liquid-phase mixing. The combustion-chamber characteristic length required to obtain 97 percent of maximum experimental characteristic exhaust velocity was used as the measure of reactivity. Hydrazine, trimethyl-trithiophosphite, furfuryl alcohol, unsymmetrical dimethylhydrazine, allylamine, and o-toluidine were studied; reactivity decreased in that order.

A swirl-cup-type injector was used. Injector spray pattern and mixing efficiency were determined. The swirl-cup pressure drop depended strongly on the nature of the fuel-acid mixture and was assumed to be a measure of the vigor of the reaction occurring in the cup.

One-inch-diameter chambers of various lengths were used. Two of the fuels were also studied in $1\frac{1}{2}$- and 2-inch-diameter chambers. Reactivities are shown to be dependent on the acid-fuel ratio. Reactivities, injector-cup pressure drops, and ignition delays are compared and discussed.

INTRODUCTION

The selection of rocket propellants for a specific purpose would be aided if, in addition to thermodynamic and physical data, there were available some index of reaction rate. Such an index would also be of value in the design of the smallest, lightest combustion chambers consistent with efficient combustion.

Several investigations have been made to determine reactivities or conversion rates in rocket combustion chambers. In one, the characteristic exhaust velocity c^* was measured as a function of chamber length for several fuels with liquid oxygen as the oxidizer (ref. 1). (The symbols used in this report are defined in appendix A.) The study was primarily for the purpose of correlating conversion rates with flame speeds and slow oxidation rates. Flame speeds and slow oxidation rates are not

necessarily related to combustion processes that occur in rocket engines; however, qualitative correlations were obtained. Similar data have also been used in the evaluation of injector configurations for the system, white fuming nitric acid (WFNA) and JP-3 fuel (ref. 2).

In another investigation the static-pressure profile along a tubular engine was determined, and from this, reaction rates were inferred (ref. 3). WFNA-ammonia and WFNA-hydrazine systems were studied with a number of injector configurations. Similar data have been interpreted to give a minimum required residence time for the combustion of gaseous methane and oxygen (ref. 4).

This report describes an investigation of the relative reactivities of several fuels with red fuming nitric acid (RFNA) under conditions where the effect of liquid-phase mixing is minimized. The combustion-chamber characteristic length L^* required to obtain 97 percent of the maximum experimental characteristic exhaust velocity c^* was used as the measure of reactivity. A swirl-cup-type injector was used because this type has been shown to produce very rapid liquid-phase mixing (ref. 5). The mixing efficiency and spray pattern of the injector were determined.

Six fuels, representative of several classes, were studied using RFNA (19 percent NO_2) as the oxidizer. The experiments were conducted in a nominal 40-pound-thrust rocket engine. The characteristic length L^* of the combustion chamber was varied by using different lengths of 1-inch-diameter pipe. Two of the fuels were also studied in $1\frac{1}{2}$- and 2-inch-diameter chambers to determine the effect of diameter on the general level of performance and on the reactivities of the fuels. The ratings of the fuels, based on data for c^* and L^* and cup pressure drop, are compared.

An attempt was made to interpret the results of this study assuming that the conversion of NO to N_2 is an important rate-determining step in the final stages of combustion involving nitric acid (refs. 6 and 7).

APPARATUS AND PROCEDURE

Rocket Engine

A cross-sectional view of the rocket engine and injector is shown in figure 1.

Injectors. - The injectors were of a swirl-cup type similar to that reported in reference 8. Propellants entered the mixing cup tangentially at an inlet angle of 10°. The cross-sectional area of the mixing cup was 4 times the sum of the cross-sectional areas of the inlet orifices. The cup length was chosen for approximately 1 millisecond of residence time based on the calculated velocity of unreacted propellants. Two injectors

with different inlet-orifice diameters were required to permit operation over a wide range of mixture ratios. The injector heads were constructed of stainless steel and contained a pressure tap leading directly to the chamber.

Separate experiments were conducted to determine the mixing efficiencies and spray patterns of the injectors. The details of these experiments are presented in appendix B. The results indicate that mixing was largely excluded as a factor in the present study and that the data represent primarily evaporation and chemical-reaction rates. Studies of the spray patterns indicated an almost uniform distribution with a cone angle of about 37°.

Chambers. - Uncooled chambers were made of extra-heavy seamless steel pipe having 1-, $1\frac{1}{2}$-, and 2-inch nominal diameters. In addition, transparent chambers of cast acrylic resin were used for a photographic study. These had a wall thickness of 1/4 inch and inside diameters of 1, $1\frac{1}{2}$, and 2 inches. Figure 1 shows a 1-inch chamber only. Adaptors were used to fit the wider chambers to the injector. When adaptors were used, there was a prechamber space 2/3-inch long with a 1-inch diameter. This space had a characteristic length of 6 inches. The 1-, $1\frac{1}{2}$-, and 2-inch-diameter chambers had characteristic lengths of 8.1, 19.9, and 33.3 inches, respectively, per inch of chamber length.

Nozzles. - Stainless-steel water-cooled nozzles having a convergent section only were used. The nozzles were constructed with steps to accommodate the various chamber diameters. The injector, chamber, and nozzle were bolted together and sealed by copper or aluminum gaskets at both ends of the chamber. The entire assembly was directed downward.

Flow System and Operation

The flow system of the test rig was similar to those used in other experimental rocket setups. The two propellant tanks could be pressurized independently to about 850 pounds per square inch gage. A pneumatically operated firing valve permitted flow of both propellants to begin simultaneously. The initial flow rates were about twice the steady-state values. Because of the high initial flow rates, the ignition process was affected and hard starts were encountered with furfuryl alcohol, allylamine, and o-toluidine. In order to prevent such hard starts, these fuels were preceded by a 3- to 5-cubic-centimeter slug of 82 percent hydrazine, which was fed directly into the firing valve through a short length of vertically mounted tubing. The other fuels showed smooth-starting characteristics over the entire range of acid-fuel ratios.

Without starting fuel the total running time was usually 1 to 2 seconds. When starting fuel was used, the running time was increased to about 3 seconds to ensure the complete removal of the starting fuel. Running time on starting fuel ranged from 0.2 to 0.5 second. Transition from starting fuel to running fuel could sometimes be detected in the flow and chamber-pressure records. All the runs were long enough so that the flow rates and chamber pressure reached constant values.

In order to purge the injector and chamber at the end of each run, high-pressure helium was automatically admitted downstream of the firing valve just as the valve closed.

Instrumentation

Duplicate measurements were made of all primary variables. Propellant flow rates were measured both by rotating-vane flowmeters and by orifices in conjunction with strain-gage differential-pressure transducers. In order to protect the pressure transducer in the acid line from the corrosive action of the acid, a fluorocarbon oil was placed in the lines connecting the orifice and the transducer chamber. The oil (sp. gr., 1.95), being heavier than acid, prevented contact between the acid and the sensitive instrument diaphragms. Although some NO_2 was absorbed by the oil, no corrosion of the metal diaphragm was observed over a period of a year.

The chamber pressure was measured by two strain-gage static-pressure transducers placed 18 and 30 inches from the injector on a single pressure tap line. The pressure tap line was 1/4-inch-diameter stainless-steel tubing and was provided with a slight helium bleed to keep it unblocked and to prevent possible explosions due to propellant entry on starting.

The outputs of all instruments were recorded on a multichannel galvanometer-type oscillograph. The flow rates and pressures used were averages of the duplicate measurements. The deviations between flow rates obtained from the rotating-vane instrument and the orifice-strain-gage combination averaged 0.003 pound per second for the acid and 0.002 pound per second for the fuel. The deviations between chamber-pressure measurements from each of the strain gages averaged 2.2 pounds per square inch.

The nozzle diameter was measured before and after each series of runs, and an average of these two values was used. Propellant temperatures were measured with a mercury thermometer at each loading of the tanks.

Fuels and Acids

The acid used throughout the study was a red fuming nitric acid containing 19 percent NO_2 and 2 percent water. The six fuels used were 92.2 percent hydrazine, commercial-grade trimethyl-trithiophosphite (TMTP), commercial-grade furfuryl alcohol, commercial-grade unsymmetrical dimethylhydrazine (UDMH), commercial-grade allylamine, and chemically pure o-toluidine. In the mixing efficiency tests, 18.8 percent HNO_3 and 18.2 percent NaOH in water were used.

Treatment of Data

The characteristic length L^* was calculated from chamber volume/nozzle throat area; characteristic exhaust velocity c^* was calculated from (chamber pressure)(nozzle throat area)/total flow rate. The L^* corresponding to maximum c^* is difficult to locate accurately because the experimental curves are almost horizontal over a wide range of L^* near the maximum. For this reason the L^* for comparison was chosen as that at which c^* reached 97 percent of its maximum value. At this point L^*_{97} the curves are steep enough to give a well-defined value of L^*.

Values of β $(o/f)/(o/f)_{stoichiometric}$ of 0.55, 0.65, 0.80, 1.0, and 1.25 were selected for comparing the various fuels. The acid-fuel weight ratios o/f corresponding to these β values are shown for each fuel in table I. The choice of these values was limited by the range of the data, which in some cases did not extend to the extreme values. Special significance is attached to β of 0.80 since it corresponds approximately to the o/f of maximum c^* for all the fuels.

Theoretical performance data for the exact acid composition used in this study were not available; however, some applicable data were found. The data for hydrazine and furfuryl alcohol are from reference 9. The data for UDMH are from reference 10. It was necessary to correct the hydrazine data for the effect of about 8 percent water. The correction was based on the data of reference 9 and reduced the c^* values for anhydrous hydrazine by 1.2 percent.

RESULTS

The basic measured and calculated data are shown in table II for each fuel. The flow-rate values are given to three decimal places; however, in some cases four places were used to compute c^* and o/f. Runs in which screaming (high-frequency sound due to combustion oscillations)

was heard are marked. In every case when screaming was heard, the chamber-pressure record was smooth and free from random disturbances otherwise present.

Figure 2 shows typical c^* - o/f curves for each fuel at the L^* giving the highest c^*. These data are for 1-inch-diameter chambers and are representative of data obtained at other L^* values. The experimental points show the reproducibility of the data to be very good. Theoretical c^* curves for three of the fuels are also shown in figure 2.

Combustion Characteristics of the Fuels

Three of the fuels, hydrazine, TMTP, and UDMH, were very smooth in operation giving no hard starts or audible screaming. Furfuryl alcohol screamed consistently in chambers having an L^* of 50 inches and greater over the entire o/f range studied. Some intermittent screaming was observed with allylamine and o-toluidine in the longer chambers. This usually occurred near the end of a run, so that it was usually possible to obtain data when there was no screaming. No difference was observed between c^* values for screaming and nonscreaming runs. This is illustrated in figure 2 where data points for both conditions are shown for furfuryl alcohol and o-toluidine. TMTP produced hard deposits in the nozzle throat. Both furfuryl alcohol and o-toludine formed copious carbon deposits in the chambers.

Fuel Ratings

In figure 3, c^* is shown as a function of L^* and o/f for each fuel. The curves are for 1-inch-diameter chambers and are taken from smoothed c^* - o/f plots like those in figure 2. The β values at which the fuels are compared later are marked. From figure 3 it can be seen that the o/f giving a maximum c^* generally increases as L^* is increased.

In figure 4, the fuels are compared at a β of 0.80; L^*_{97} points are shown. These curves are similar in form to those obtained at the other values of β. The characteristic exhaust velocities c^* for allylamine and o-toluidine did not reach a maximum even at an L^* of 100 inches. As an approximation, maximum c^* was taken as that at an L^* of 100 inches; therefore the L^*_{97} values are a minimum for these two fuels. The results of the evaluation of L^*_{97} are given in table III as a function of β for the six fuels. The maximum c^* values are listed in table IV.

The fuels in order of increasing L^*_{97} and hence decreasing reactivity are hydrazine, TMTP, furfuryl alcohol, UDMH, allylamine, and o-toluidine.

It is apparent from table III that the reactivity decreases as the stoichiometric o/f increases. On the fuel rich side, the L^*_{97} values generally increase for a given fuel as β increases. The dependence on the relative amounts of acid and fuel present is shown in figure 5 in which all of the L^*_{97} values in table III are plotted against the corresponding o/f. The data fall into two groups with allylamine and o-toluidine separated from the remaining four fuels.

Pressure in the Mixing Cup

The flow rates observed during live runs were much lower than those expected from cold-flow tests. This effect was apparently due to a large pressure drop in the injector mixing cup resulting from liquid-phase reaction. Cup pressure drop is a measure of the amount of liquid-phase reaction in the cup, since only a negligible pressure drop would have resulted from fluid friction alone. The cup pressure drop was calculated using the equation for flow through an orifice. Details of the calculation are given in appendix C. Calculated values of the cup pressure drop are shown in figure 6 as a function of o/f. The values are corrected to a uniform flow rate of 0.2 pound per second (see appendix C). The pressure drops tend toward a common value independent of the fuel as o/f is increased.

Effect of Chamber Diameter

The effect of chamber diameter on the general level of performance and on the reactivities of the fuels was investigated. Two fuels, hydrazine and UDMH, showing widely different reactivities in the 1-inch-diameter chambers were studied in $1\frac{1}{2}$- and 2-inch-diameter chambers. Characteristic exhaust velocity c^* for each diameter is shown as a function of L^* in figure 7(a) and as a function of chamber length in figure 7(b). Data for β equal to 0.80 only are shown as they are typical of the data for all β values. From figure 7(a), the L^* corresponding to maximum c^* increased with diameter for both fuels. From figure 7(b) the chamber length corresponding to maximum c^* decreased with diameter for UDMH, while no trend was observed for hydrazine. The maximum c^* increased slightly with diameter for UDMH, while no trend was observed for hydrazine.

L^*_{97} values are shown in table V as functions of diameter for hydrazine and UDMH. L^*_{97} increases with both diameter and β.

DISCUSSION

Effect of Chamber Diameter

An analysis of the data of table V showed that an essentially constant difference exists between the L_{97}^* values of each of the larger chambers and the 1-inch chambers. The average differences in L_{97}^* values, shown in table VI, are 19.1 inches between the $1\frac{1}{2}$- and 1-inch diameters and 42.9 inches between the 2- and 1-inch diameters. As discussed in appendix B, the injectors produced a conical spray pattern. It was assumed that the chamber volume outside the spray cone did not contribute to the effective combustion volume. This ineffective combustion volume was calculated from the cone angle and chamber geometry. The ineffective volume was converted to an equivalent L^* for each of the chamber diameters. The difference in L^* values thus obtained for the various chamber diameters were of the same order of magnitude as those observed experimentally. The differences may be applied as a correction to the L_{97}^* values obtained with the larger-diameter chambers resulting in approximately the same L_{97}^* values for all diameters. This result indicates that in the range of diameters studied there is little effect of chamber diameter on the observed reactivities.

Correlation of Reactivity with Initial NO Concentration

From the relation between L_{97}^* and o/f shown in figure 5, it appears that, in a very general way, the reactivity of a combination containing unit mass of fuel depends on the amount of acid present; that is, even on the fuel rich side, the reactivity decreases as the acid concentration is increased. For some of the fuels the differences in reactivity between fuels were less than those produced by changes in the acid-fuel ratio. It seems reasonable therefore to relate reactivity to some function of acid concentration in the reactant mixture.

It has been postulated that in oxidation reactions involving nitric acid or NO_2, where NO is an intermediate, the steps involving NO are slow and rate-determining. It has been found that the measured flame speeds of NO-hydrocarbon mixtures were about 1/10 those of oxygen-hydrocarbon mixtures with hydrocarbons such as ethane, ethylene, and acetylene (ref. 11). Other evidence indicates that higher temperatures are required to propagate NO supported flames than flames supported by O_2 or NO_2 (ref. 12). Also, analysis of the primary cone of a premixed gaseous nitric acid-hydrocarbon flame showed that nearly all the nitrogen is recovered as NO (ref. 13).

An attempt was therefore made to correlate the experimental data with some function of NO concentration. It was assumed that the following reaction occurs very rapidly to form intermediates and products as shown:

$$\text{Fuel} + HNO_3\ (NO_2) \rightarrow NO + CO_2 + CO + C + H_2O + H_2 + N_2 + P_2O_5 + SO_2$$

All the nitrogen in the acid has been assumed to form NO. The other species are formed, where applicable, from the fuel. For each mixture ratio, the initial mole fraction of NO (moles NO/total moles) was calculated. Whether CO_2, CO, or C and H_2O or H_2 is formed is not known but has no effect on the total number of moles. It was necessary, however, to assume that the amounts of O_2, OH, H, CH, and so forth present after the initial reaction are negligible. Using experimental chamber pressures each mole fraction was converted to a partial pressure of NO. The initial partial pressure of NO represents the amount of NO that must react to carry the reaction to completion. These pressures are plotted as a function of L^*_{97}/c^*_{97} for each fuel in figure 8. The ratio L^*_{97}/c^*_{97} has the dimensions of time and is shown in appendix D to be roughly proportional to the residence time of the propellants from injection to the point of 97 percent maximum c^*.

The shapes of the curves for the individual fuels in figure 8, with the possible exception of hydrazine, are inconsistent with any rate law based on a single reaction. If, at the final state (97 percent maximum c^*), the partial pressure of NO is the same value for all mixtures, and if the disappearance of NO followed a first, second, or higher order dependence, the curves would be concave to the pressure axis.

The curves for furfuryl alcohol, UDMH, and allylamine approach a common limiting line at higher initial NO concentrations. The slope of the limiting line is small and may represent the thermal decomposition of NO. At lower initial NO concentrations the slopes are higher suggesting that NO is reacting with fuel fragments. Thus the shape of the curves may be explained on the basis of two competing reactions, one, the thermal decomposition of NO, which is slower, and the other, the reaction of NO with fuel fragments, which is faster. The curve for hydrazine does not suggest such a mechanism; however, the initial partial pressures of NO in all runs with hydrazine were quite low. The TMTP and o-toluidine curves are not consistent with such a conclusion.

The slope of the limiting line in figure 8 was found to be 3.9×10^3 pounds per square inch per second. The calculation of the slope includes a correction of the time base of figure 8 as shown in appendix D. The rate of thermal decomposition of NO, calculated from experimental data, increased from 6.5×10^3 to 4.6×10^4 pounds per square inch per second as the temperature was increased from 3500° to 4100° R (ref. 6). Thus the slope of the limiting line is of the same order of magnitude as the calculated rate of thermal decomposition of NO.

The validity of this correlation is, of course, limited by the uncertainty of the final concentration of NO and the assumptions regarding the fate of the fuel atoms.

Comparison of Cup Pressure-Drop, L_{97}^*, and Ignition-Delay Values

The values of the steady-state pressure drop in the mixing cup were shown in figure 6 as a function of o/f for each fuel. The propellants are in the mixing cup for about 1 millisecond so that a high cup pressure drop indicates appreciable early reaction. From figure 6 it is apparent that the pressure drop is fuel dependent for fuel-rich mixtures. Cup-pressure-drop values and L_{97}^* values are compared at a β of 0.65 in table VII. With the exception of furfuryl alcohol, cup-pressure-drop ratings follow the same trend as L_{97}^* ratings.

The ignition-delay values of the fuels also shown in table VII were not all obtained under comparable conditions; however in general, the fuels are divided into two groups according to their ignition delays. Fuels having short ignition delays, hydrazine, TMTP, and UDMH, have the highest cup-pressure-drop values. Fuels having long ignition delays have the lowest cup-pressure-drop values.

It is to be expected that cup pressure drops and ignition delays should correlate because both characterize the initial processes in the combustion reaction. However, L_{97}^* is a measure of the over-all conversion rate and characterizes the entire combustion process. Moreover, the correlation with initial NO concentration suggests that L_{97}^* may be largely determined by the final stages of the combustion process. The observation that L_{97}^* ratings and cup-pressure-drop ratings follow the same trend indicates that generally a combustion reaction which is vigorous in its early stages also will have a high over-all conversion rate.

As shown in figure 6, the cup-pressure-drop values for all the fuels seem to approach a common value of about 80 pounds per square inch at high o/f ratios. This value is considerably higher than would be expected from fluid friction alone. It may be due to thermal decomposition of the acid, with the necessary heat being supplied by transfer upstream from the combustion process. If it were caused entirely by reaction of fuel and acid in the cup, it would be expected that different values would be obtained for the various fuels such as were obtained at lower o/f ratios.

Over-All Combustion Efficiency

Theoretical performance curves for three of the fuels were shown in figure 2. The following table shows the percent of theoretical c^* obtained at the o/f of experimental peak c^*.

Fuel	L^*	Percent of theoretical c^*	
		Frozen expansion	Equilibrium expansion
Hydrazine	40	92.4	----
Furfuryl alcohol	50	94.3	90.5
UDMH	75	----	90.6

As discussed previously, the acid composition used in the calculation of theoretical c^* did not correspond exactly to that used in the experimental study. Within this limitation the experimental efficiency is about the same for all three fuels. The experimental data are uncorrected for heat lost to the walls. An estimate of such heat loss showed that it could vary from about 3 percent in an L^* of 30 inches to about 8 percent in an L^* of 100 inches for the 1-inch-diameter chambers. It appears therefore that the relatively low efficiency can be largely accounted for by heat transfer to the chamber walls.

CONCLUDING REMARKS

The concept of a volume required to complete a reaction has been used to classify six fuels with respect to their reactivities. The importance of data of this kind can be illustrated by the results of some performance measurements on a 5000-pound-thrust NH_3-RFNA engine having an L^* of 17.5 inches (ref. 14). In spite of the small L^*, high specific impulse was obtained indicating that NH_3 has a high reactivity. The effect of adding UDMH to the NH_3 was then studied. Although UDMH has a higher theoretical performance than NH_3, the addition of 30 percent UDMH to the NH_3 lowered the specific impulse 13 percent. This is not surprising in the light of the present research since an L^* of about 75 inches was required to obtain maximum performance with UDMH.

It is possible that finer discrimination between fuel-oxidant systems could be obtained by using a continuously variable L^* engine. This would improve the internal consistency of the data by eliminating cross plots. It would also allow the entire L^* range to be scanned.

SUMMARY OF RESULTS

Using the chamber characteristic length L^* required to obtain 97 percent of maximum experimental characteristic exhaust velocity c^* as an index, the relative reactivities of six fuels with RFNA were determined. The experiments were conducted in a 40-pound-thrust rocket engine using a swirl-cup injector which gave about 70-percent-complete liquid-phase mixing. The results of the investigation may be summarized as follows:

1. The reactivities of the fuels were found to decrease in the following order: Hydrazine, trimethyl-trithiophosphite, furfuryl alcohol, unsymmetrical dimethylhydrazine, allylamine, and o-toluidine. The latter two fuels had considerably lower reactivities than the remaining four fuels.

2. As acid-fuel ratio o/f was increased, the reactivities of the fuels generally decreased.

3. From an analysis of the effect of stoichiometry, it appears that for at least three of the fuels two reactions involving NO may be important. The reaction of NO with fuel fragments is the faster reaction; the thermal decomposition of NO is slower.

4. The pressure drop through the mixing cup appeared to be a measure of the extent of liquid-phase reaction. This pressure drop followed the same general trend as ignition delay.

5. The chamber diameter had no effect on the relative ratings of two fuels studied as functions of diameter.

Lewis Flight Propulsion Laboratory
National Advisory Committee for Aeronautics
Cleveland, Ohio, January 19, 1956

APPENDIX A

The following symbols are used in this report:

A	area, sq in.
C_d	discharge coefficient
c^*	characteristic exhaust velocity, $p_c A_t g/w_t$, ft/sec
g	gravitational constant, 32.2 ft/sec^2
h	ratio of average value of RT/M to value at nozzle entrance
K	flow constant, $C_d^2 A^2 2g\rho/144$, (lb)(sq in.)/sec^2
L^*	characteristic length, V_c/A_t, in.
M	molecular weight of combustion gases
o/f	acid-fuel ratio, w_o/w_f
p	pressure, lb/sq in.
R	universal gas constant, ft-lb/lb-mole $^\circ$R
T	combustion-chamber temperature, $^\circ$R
t	residence time of combustion gases in chamber, sec
V_c	combustion-chamber volume, cu in.
V_g	average specific volume of gases in combustion chamber, cu ft/lb
w	flow rate, lb/sec
w_T	total flow rate, $w_o + w_f$, lb/sec
β	weight fraction of stoichiometric o/f, $\frac{o/f}{(o/f)_{stoichiometric}}$
Γ	$\gamma\sqrt{\left(\frac{2}{\gamma+1}\right)^{\frac{\gamma+1}{\gamma-1}}}$
γ	specific-heat ratio
ρ	density, lb/cu ft

Subscripts:

av	average
c	combustion chamber
cup	injector mixing cup
f	fuel
i	nozzle inlet
o	acid
p	propellant tank
t	nozzle throat

APPENDIX B

INJECTOR CHARACTERISTICS

The injector was characterized by studies of its mixing efficiency and spray pattern.

Mixer

A separate apparatus (fig. 9) was used to study the mixing efficiency of the injector. The flow arrangement was identical to that in the injector except that the mixing cup was extended to a length of 6 inches with tubing having a 0.020-inch wall thickness. Iron-constantan thermocouples were spot-welded to the mixing tube at various stations. The entire mixer was enclosed by a heater so that the initial temperature of the block, which is the greatest heat sink, could be adjusted to minimize heat transfer. The extended tube was carefully insulated from the heater to avoid heat transfer from the heater to the mixing tube during a run.

Efficiency of Mixing

The mixing efficiency of the injector was studied with dilute nitric acid and sodium hydroxide. Inasmuch as the reaction between a strong base and a strong acid is instantaneous and dependent only on the rate of mixing (ref. 5), the heat evolved by such a reaction can be used as an index of the completeness of mixing under adiabatic conditions. By following the temperature rise as a function of distance along the mixing tube, mixing efficiency can be determined (ref. 5). The temperature corresponding to complete mixing is calculable from thermodynamic data.

Smoothed data with three initial block temperatures are shown in figure 10. The upper curve corresponds to a high initial block temperature, which caused heat to be added to the stream resulting in a final temperature well above theoretical. The lower curve corresponds to a low initial block temperature for which the final temperature is below theoretical. The middle curve closely approximates the adiabatic case since the final temperature does reach theoretical. This is substantiated by the fact that the initial block temperature seems to be a reasonable average of the stream temperature in the region of the large block. From this curve it can be deduced that it requires 2.2 inches to achieve 97-percent-complete mixing. The extent of mixing at the distance corresponding to the end of the mixing cup in the rocket injector was found to be 70 percent. Whether the efficiency measured in the test mixer can be applied to mixing in the injector, under conditions where large amounts of heat and gas are evolved, may be somewhat questionable. A similar mixer,

under these conditions, gave an essentially complete reaction as fast as the reactants emerged from the mixer (ref. 15). It is thus concluded that mixing is largely excluded as a factor in the present study and that the data represent primarily evaporation and chemical-conversion rates.

Studies of Spray Pattern

Experiments were conducted with plastic chambers of three diameters to determine how the reactants leaving the injector entered the chamber. Erosion patterns of the chambers using hydrazine as the fuel are shown in figure 11. The diameter measurements shown are averages of those made at a given station for two radial positions at right angles. The data for both positions are shown for the 2-inch chamber. Erosion was nearly symmetric about the circumference of the chamber indicating an almost uniform spray distribution.

The point of maximum erosion moved away from the injector as the diameter was increased. It was assumed that the point of maximum erosion represents the point of impingement of the burning spray from the injector on the chamber walls. These points are shown on a sketch of the chambers in figure 11. It can be seen that a straight line connecting them can be extended to the vicinity of the injector cup. This indicates that the injector spray under operating conditions is a cone having an included angle of about 37°. High-speed motion pictures, made with a framing camera, of the steady-state combustion showed that the chambers were not filled by luminous flame and that the cone angle was of the order of 40°. High-speed streak photographs showed considerable recirculation in the vicinity of the injector. Cold-flow tests using water gave a hollow-cone spray with an included angle of about 60°.

These results indicate that at least a part of the chamber volume upstream of the cone of burning may not contribute to the effective combustion volume.

APPENDIX C

CALCULATION OF PRESSURE DROP IN THE MIXING CUP

The calculation of cup pressure drop is possible because the mixing cup is the first point common to both the fuel and the acid flow lines. The calculation is based on the equation for orifice flow

$$w = C_d A \sqrt{\frac{2g\rho\Delta p}{144}} \tag{C1}$$

If the friction factor is assumed constant, equation (C1) may be applied to the entire flow line. Equation (C1) may be squared and written both for the fuel line and the oxidant line as follows:

$$w_f^2 = K_f (p_{f,p} - p_{cup}) \tag{C2}$$

$$w_o^2 = K_o (p_{o,p} - p_{cup}) \tag{C3}$$

where $p_{f,p}$ and $p_{o,p}$ are the fuel and oxidant tank pressures, respectively. Eliminating p_{cup} from equation (C2) and (C3),

$$\frac{w_o^2}{K_o} - \frac{w_f^2}{K_f} = p_{o,p} - p_{f,p} \tag{C4}$$

Dividing by w_f^2 and rearranging give

$$\frac{p_{o,p} - p_{f,p}}{w_f^2} = \frac{(o/f)^2}{K_o} - \frac{1}{K_f} \tag{C5}$$

When $(p_{o,p} - p_{f,p})/w_f^2$ is plotted against $(o/f)^2$, equation (C5) is a straight line of slope $1/K_o$ and intercept $-1/K_f$.

The experimental program was conducted at a number, usually eight, of tank pressure settings for each fuel at each of the characteristic lengths studied. The experimental values of w_o, w_f, and p_c obtained with the various characteristic lengths at given tank pressure settings were averaged. The tank pressure settings and the average of each of the observed flow rates were then used to plot equation (C5). Such a plot for hydrazine is shown in figure 12. The corresponding plots for the other fuels also gave straight lines. From the measured slope and intercept, values of K_o and K_f were determined. K_o, K_f, $p_{f,p}$, $p_{o,p}$, w_f,

and w_o being known, p_{cup} was calculated from equations (C2) and (C3). The two values of p_{cup} agreed very closely, and their average was used to calculate the pressure drop by subtracting the chamber pressure from it;

$$\Delta p_{cup} = p_{cup} - p_c \tag{C6}$$

Since the average total flow rate w_T was not the same for each fuel, the cup-pressure-drop values were corrected to a common flow rate of 0.2 pound per second. In the absence of data on the flow of reacting mixtures the cup-pressure-drop values were assumed proportional to the total flow rate and adjusted to the reference value as follows:

$$\Delta p_{cup,0.2} = \frac{0.2}{w_T} \Delta p_{cup,w_T} \tag{C7}$$

This constituted a relatively minor correction except in the case of hydrazine where the total flow rates were relatively low. The application of equation (C7) did not, however, change the relative order of the results.

APPENDIX D

RESIDENCE TIME IN CHAMBER

The residence time is given by equation (6-4) of reference 16

$$t = \frac{V_c}{w_T V_g} \tag{D1}$$

V_g may be eliminated from equation (D1) by using the perfect gas law $V_g = (RT/M)_{av}/p_c$ to give

$$t = \frac{p_c V_c}{w_T (RT/M)_{av}} \tag{D2}$$

Since $c^* = p_c A_t g/w_T$ and $L^* = V_c/A_t$,

$$t = L^* c^* \frac{1}{g(RT/M)_{av}} \tag{D3}$$

The $(RT/M)_{av}$ term is an average value for the entire chamber. It may be eliminated from equation (D3) by making use of an alternate expression for c^*, equation (3-32) of reference 16,

$$c^* = \frac{\sqrt{g\gamma(RT/M)_i}}{\Gamma} \tag{D4}$$

The $(RT/M)_i$ in equation (D4) refers to conditions at the nozzle entrance. The c^* and L^* values involved in figure 8 refer to 97 percent maximum c^*. Because of the general similarity between the $c^* - L^*$ curves for different fuels, it is reasonable to assume that $(RT/M)_{av}$ is equal to the same fraction of $(RT/M)_i$ for all cases since the nozzle conditions in all cases are comparable. Hence

$$(RT/M)_{av} = h(RT/M)_i \tag{D5}$$

where h is a constant.

Combining equations (D3), (D4), and (D5) yields

$$t = \frac{L^*}{c^*} \frac{\gamma}{h\Gamma^2}$$

The value of γ/Γ^2 is rather insensitive to the value of γ chosen. For γ values between 1.10 and 1.60, γ/Γ^2 varies from 2.53 to 1.95. A value of 2.3 for γ/Γ^2 was used. A value of unity was chosen for h. A value of h as low as 0.5 is unlikely; however, such a value would halve the rate obtained from the limiting line in figure 8.

REFERENCES

1. Raines, T., and Pisani, J.: Combustion Kinetics Investigation. Rep. RMI-487-F, Final Rep., Reaction Motors, Inc., Dec. 30, 1953. (Contract NOas 53-406-c.)

2. Datner, P. P., and Dawson, E. E.: Testing of Repetitive-Pattern Injectors in 1000-Lb Thrust Chambers with Chamber-to-Throat Area Ratios of 4.5 Using WFNA and JP-3. Rep. 555, Aerojet Eng. Corp., July 25, 1952. (Contract AF 33(038)-2733, Proj. MX-1079, E.O. No. 539-44.)

3. Samek, M. J., Baldwin, R. R., Cinnirella, E. O., and Kalil, E. O.: Combustion Kinetics in a Tube Motor. Rep. SPD 313, Final Rep., Special Proj. Dept., The M. W. Kellogg Co., Sept. 15, 1951. (Contract NOrd-10768 for U.S. Navy, Bur. Ord.)

4. Charyk, J. V., and Matthews, G. B.: Experimental Studies of Energy Release Rates in Rocket Motor Combustion Chambers. Rep. No. 191, Dept. Aero. Eng., Princeton Univ., Mar. 24, 1952. (Contract N6-ori-105, Task Order III, NR 220-038.)

5. Roughton, F. J. W., and Chance, B.: Investigation of Rates and Mechanisms of Reactions. Vol. 8 of Technique of Organic Chemistry, A. Weissberger, ed., Interscience Publ., 1953, p. 669.

6. Trent, C. H., and Datner, P. P.: A Study of Combustion of WFNA and JP-3 in Rocket Thrust Chambers. Rep. No. 628, Aerojet Eng. Corp., Nov. 15, 1952. (Contract AF 33(038)-2733, Item 30, Proj. MX-1079, E.O. No. 539-44.)

7. Wise, Henry, and Frech, Maurice F.: Reaction Kinetics of Rocket Propellant Gases. I. Rate of Decomposition of Nitric Oxide at Elevated Temperatures. Prog. Rep. No. 9-46, Jet Prop. Lab., C.I.T., Mar. 27, 1950. (Proj. No. TU2-1, Contract No. W-04-200-ORD-1482.)

8. Fredrickson, H., and Rice, P. J.: Second Progress Report on Rocket Motor Throttling. UMM-89, Eng. Res. Inst., Willow Run Res. Center, Univ. Mich., Jan. 1952. (USAF Contract W33-038-ac-14222, Proj. MX-794.)

9. Anon.: 6000 Pound Thrust Jet Propulsion Unit. Pt. I - Propellants Study. Final Rep., SPD-134, Spec. Proj. Dept., The M. W. Kellogg Co., Mar. 19, 1948. (USAAF Contract No. W-33-038-ac-13916.)

10. Camp, Clarence: Experimental Performance of Unsymmetrical Dimethylhydrazine Red Fuming Nitric Acid Rocket Propellant Combination. WADC Tech. Rep. 54-81, Wright Air Dev. Center, Wright-Patterson Air Force Base, Feb. 1954.

11. Parker, W. G., and Wolfhard, H. G.: Some Characteristics of Flames Supported by NO and NO_2. Fourth Symposium (International) on Combustion, The Williams & Wilkins Co. (Baltimore), 1953, pp. 420-428.

12. Miller, Riley O.: Flame Propagation Limits of Propane and n-Pentane in Oxides of Nitrogen. NACA TN 3520, 1955.

13. Propulsion Engineering: Bimonthly Progress Report on the Improvement of White Fuming Nitric Acid. Rep. RE-16-12, North American Aviation, Inc., July 22, 1955. (Contract AF 33(616)-329.)

14. Special Products Research Department: Small Caliber High Performance Liquid Fueled Rocket Motor. Prog. Rep. No. 10, Rep. No. 80-4450R, Eclipse-Pioneer Div., Bendix Aviation Corp., July-Aug. 1954. (Contract No. W-30-069-ORD-4450R, Ord. Proj. TU2-7C.)

15. Kilpatrick, Martin, Baker, Louis L., Jr., and McKinney, C. Dana: Studies of Fast Reactions Which Evolve Gases. The Reaction of Sodium-Potassium Alloy with Water in the Presence and Absence of Oxygen. Jour. Phys. Chem., vol. 57, no. 4, Apr. 16, 1953, pp. 385-390.

16. Sutton, George P.: Rocket Propulsion Elements. John Wiley & Sons, Inc., 1949.

17. Ladanyi, Dezso J., and Miller, Riley O.: Comparison of Ignition Delays of Several Propellant Combinations Obtained with Modified Open-Cup and Small-Scale Rocket Engine Apparatus. NACA RM E53D03, 1953.

18. Carmody, D. R., and Zletz, A.: Development of Liquid Rocket Propellants. Final Rep., Standard Oil Co. (Ind.), May 15, 1954. (Contract AF-33(038)-22633.)

19. Strier, M., Felberg, R., and Pearl, C.: Investigation of the Relationship of Propellant Chemical Structure to Spontaneous Ignition with WFNA. Final Rep. No. RMI-466-F, Reaction Motors, Inc., Mar. 23, 1953. (Contract NOa(s)52-595-c.)

TABLE I. - ACID-FUEL RATIOS CORRESPONDING TO VARIOUS β VALUES

Fuel	Acid-fuel ratio o/f for β^a of -				
	0.55	0.65	0.80	1.00	1.25
Hydrazine	----	0.96	1.18	1.48	1.85
TMTP	----	1.82	2.24	2.80	3.50
Furfuryl alcohol	----	1.85	2.28	2.85	3.56
UDMH	1.86	2.20	2.70	3.38	----
Allylamine	2.33	2.75	3.38	4.23	----
o-Toluidine	2.41	2.85	3.50	4.38	----

[a] $\left[\frac{(o/f)}{(o/f)_{stoichiometric}}\right]$

TABLE II. - BASIC EXPERIMENTAL DATA

[1-in. diam. chamber used except where noted]

Chamber pressure, p_c, lb/sq in. abs	Acid flow, w_o, lb/sec	Fuel flow, w_f, lb/sec	Acid-fuel weight ratio, o/f	Characteristic exhaust velocity, c*, ft/sec	Chamber pressure, p_c, lb/sq in. abs	Acid flow, w_o, lb/sec	Fuel flow, w_f, lb/sec	Acid-fuel weight ratio, o/f	Characteristic exhaust velocity, c*, ft/sec	Chamber pressure, p_c, lb/sq in. abs	Acid flow, w_o, lb/sec	Fuel flow, w_f, lb/sec	Acid-fuel weight ratio, o/f	Characteristic exhaust velocity, c*, ft/sec
Hydrazine; A_t = 0.0882 sq in.														
L*, 10 in.					L*, 20 in.					L*, 30 in.				
201	0.055	0.072	0.77	4510	190	0.046	0.072	0.64	4550	192	0.049	0.071	0.69	4560
206	.063	.068	.92	4460	204	.056	.067	.83	4720	207	.057	.066	.87	4770
207	.069	.064	1.08	4410	219	.065	.063	1.02	4860	227	.067	.064	1.04	4930
235	.090	.064	1.41	4320	249	.083	.063	1.33	4810	246	.080	.061	1.32	4970
254	.109	.064	1.69	4170	271	.102	.061	1.67	4710	266	.094	.061	1.55	4895
267	.121	.066	1.85	4065	282	.114	.061	1.89	4570	279	.106	.060	1.76	4780
261	.126	.061	2.07	3985	279	.122	.057	2.13	4410	276	.113	.057	1.99	4610
247	.130	.055	2.35	3790	271	.130	.054	2.43	4200	266	.120	.054	2.24	4330
L*, 40 in.					L*, 50 in.					L*, 75 in.				
218	0.058	0.074	0.78	4695	244	0.068	0.075	0.90	4880	236	0.065	0.077	0.85	4730
228	.064	.068	.94	4890	250	.073	.071	1.02	4940	204	.058	.069	.85	4570
256	.080	.067	1.18	4950	253	.076	.068	1.11	5000	241	.072	.069	1.05	4865
270	.089	.064	1.37	5020	275	.089	.067	1.33	4990	263	.085	.066	1.29	4940
270	.094	.062	1.53	4920	285	.100	.066	1.53	4890	268	.093	.063	1.47	4870
282	.109	.060	1.81	4745	293	.109	.063	1.73	4840	287	.106	.063	1.69	4820
277	.116	.057	2.04	4540	279	.114	.059	1.92	4580	290	.119	.061	1.94	4590
262	.121	.052	2.33	4310	275	.119	.056	2.13	4480	272	.119	.057	2.11	4390
L*, 100 in.														
237	0.068	0.076	0.90	4665										
235	.070	.072	.98	4690										
248	.078	.070	1.11	4770										
257	.086	.067	1.30	4770										
253	.089	.063	1.42	4720										
268	.100	.062	1.63	4700										
283	.118	.062	1.92	4470										
278	.126	.058	2.17	4280										
Trimethyl-trithiophosphite; A_t = 0.0881 sq in.														
L*, 20 in.					L*, 30 in.					L*, 40 in.				
235	0.105	0.073	1.44	3750	242	0.104	0.073	1.42	3880	244	0.104	0.073	1.42	3910
248	.112	.070	1.60	3865	259	.116	.072	1.62	3930	255	.113	.072	1.59	3900
268	.128	.069	1.85	3875	271	.125	.068	1.82	3990	276	.126	.069	1.83	4020
268	.130	.064	2.03	3925	273	.129	.063	2.05	4030	281	.131	.063	2.08	4110
273	.134	.057	2.35	4050	274	.134	.057	2.35	4075	275	.132	.057	2.32	4130
271	.141	.050	2.81	4030	274	.139	.051	2.73	4090	275	.137	.052	2.63	4150
253	.145	.044	3.30	3800	259	.143	.043	3.32	3970	261	.143	.043	3.31	4010
257	.158	.043	3.67	3620	265	.153	.041	3.73	3880	267	.154	.042	3.66	3870
L*, 50 in.					L*, 75 in.					L*, 100 in.				
237	0.102	0.073	1.40	3840	234	0.103	0.074	1.40	3750	236	0.105	0.073	1.43	3770
261	.114	.072	1.58	3980	257	.117	.071	1.65	3880	255	.118	.071	1.66	3820
276	.126	.069	1.82	4040	268	.125	.068	1.84	3940	271	.128	.068	1.89	3940
277	.129	.064	2.01	4090	276	.131	.063	2.07	4000	277	.133	.063	2.10	4010
279	.132	.057	2.31	4210	274	.130	.058	2.25	4130	272	.134	.057	2.34	4050
272	.136	.050	2.72	4140	271	.135	.051	2.64	4150	271	.138	.050	2.76	4090
262	.142	.043	3.30	4010	263	.144	.042	3.42	4010	262	.142	.043	3.30	4030
270	.154	.041	3.76	3920	271	.153	.040	3.59	3975	271	.154	.041	3.76	3945

TABLE II. - Continued. BASIC EXPERIMENTAL DATA

[1-in. diam. chamber used except where noted]

Series of runs	Chamber pressure, p_c, lb/sq in. abs	Acid flow, w_o, lb/sec	Fuel flow, w_f, lb/sec	Acid-fuel weight ratio, o/f	Characteristic exhaust velocity, c*, ft/sec	Chamber pressure, p_c, lb/sq in. abs	Acid flow, w_o, lb/sec	Fuel flow, w_f, lb/sec	Acid-fuel weight ratio, o/f	Characteristic exhaust velocity, c*, ft/sec	Chamber pressure, p_c, lb/sq in. abs	Acid flow, w_o, lb/sec	Fuel flow, w_f, lb/sec	Acid-fuel weight ratio, o/f	Characteristic exhaust velocity, c*, ft/sec
	Furfuryl alcohol; A_t = [a]0.0881 and [b]0.0913 sq in.														
	L*, 20 in.					L*, 30 in.					L*, 40 in.				
1	285	0.122	0.078	1.57	4050	296	0.118	0.078	1.50	4290	298	0.115	0.078	1.47	4390
	294	.129	.074	1.76	4120	310	.125	.075	1.67	4400	311	.124	.074	1.68	4470
	313	.138	.073	1.89	4210	330	.136	.073	1.87	4490	332	.133	.073	1.83	4590
	302	.142	.068	2.09	4080	312	.134	.065	2.06	4430	321	.134	.066	2.04	4560
	289	.142	.059	2.41	4080	303	.140	.060	2.34	4300	299	.130	.056	2.32	4560
	269	.148	.055	2.69	3760	286	.146	.053	2.76	4080	293	.136	.051	2.69	4450
	246	.157	.049	3.20	3390	260	.150	.047	3.17	3740	255	.156	.040	3.92	3700
	246	.165	.049	3.37	3260	271	.160	.046	3.46	3720	272	.161	.044	3.63	3760
2	288	.129	.091	1.42	3850	302	.124	.090	1.38	4150	294	.130	.084	1.54	[c]4040
	308	.140	.092	1.52	3900	325	.133	.088	1.51	4320	321	.133	.079	1.69	[c]4450
	320	.150	.087	1.72	3970	342	.142	.084	1.69	4450	339	.142	.077	1.84	[c]4550
	294	.158	.083	1.90	3590	341	.144	.076	1.89	4560	332	.147	.070	2.10	4500
	275	.163	.078	2.40	3355	331	.148	.069	2.14	4585	327	.150	.063	2.38	4510
	299	.157	.064	2.45	3980	315	.151	.061	2.48	4370	324	.152	.059	2.58	4510
	270	.162	.059	2.74	3590	306	.153	.055	2.78	4325	314	.153	.054	2.83	4460
	274	.179	.054	3.31	3460	287	.175	.051	3.43	3730	302	.172	.050	3.44	4000
	L*, 50 in.					L*, 75 in.					L*, 100 in.				
1	258	0.096	0.084	1.15	[c]4080	302	0.119	0.073	1.63	[c]4430	289	0.117	0.075	1.56	[c]4270
	275	.104	.079	1.32	[c]4280	310	.126	.070	1.80	[c]4490	304	.126	.071	1.77	[c]4400
	321	.130	.074	1.76	[c]4480	328	.131	.067	1.96	[c]4700	313	.131	.067	1.96	[c]4490
	312	.129	.063	2.05	[c]4600	328	.135	.060	2.25	[c]4770	307	.134	.060	2.23	[c]4490
	306	.133	.057	2.34	[c]4560	309	.137	.054	2.53	[c]4590	313	.141	.054	2.62	[c]4555
	303	.136	.051	2.67	[c]4600	307	.145	.049	2.95	4490	309	.142	.049	2.91	[c]4590
	285	.142	.041	3.44	[c]4410	289	.146	.041	3.57	4390	285	.149	.041	3.63	[c]4260
	287	.154	.040	3.89	[c]4215	280	.159	.039	4.09	4010	283	.158	.040	3.95	[c]4060
2	302	.123	.082	1.51	[c]4330	288	.121	.069	1.76	[c]4460	288	.119	.077	1.54	[c]4320
	322	.133	.080	1.67	[c]4440	314	.135	.065	2.08	[c]4620	306	.131	.073	1.79	[c]4410
	344	.141	.076	1.85	4660	323	.144	.064	2.26	[c]4565	326	.142	.071	1.99	[c]4500
	336	.145	.069	2.11	4620	324	.147	.060	2.44	[c]4600	322	.143	.065	2.21	[c]4550
	326	.147	.062	2.36	4590	319	.149	.056	2.68	[c]4575	308	.145	.056	2.61	[c]4505
	315	.151	.054	2.80	4520	308	.152	.048	3.14	[c]4530	305	.149	.050	3.01	[c]4510
	298	.159	.047	3.39	4250	302	.156	.045	3.50	[c]4420	285	.156	.041	3.78	[c]4250
	305	.170	.043	3.94	[c]4210	313	.174	.044	4.00	[c]4220	268	.178	.039	4.61	[c]3630

[a]First series of runs.

[b]Second series of runs.

[c]Audible scream.

TABLE II. - Continued. BASIC EXPERIMENTAL DATA

[1-in. diam. chamber used except where noted]

Series of runs	Chamber pressure, p_c, lb/sq in. abs	Acid flow, w_o, lb/sec	Fuel flow, w_f, lb/sec	Acid-fuel weight ratio, o/f	Characteristic exhaust velocity, c*, ft/sec	Chamber pressure, p_c, lb/sq in. abs	Acid flow, w_o, lb/sec	Fuel flow, w_f, lb/sec	Acid-fuel weight ratio, o/f	Characteristic exhaust velocity, c*, ft/sec	Chamber pressure, p_c, lb/sq in. abs	Acid flow, w_o, lb/sec	Fuel flow, w_f, lb/sec	Acid-fuel weight ratio, o/f	Characteristic exhaust velocity, c*, ft/sec
	Unsymmetrical dimethylhydrazine; A_t = [a]0.0892 and [b]0.0866 sq in.														
	L*, 20 in.					L*, 30 in.					L*, 40 in.				
1	260	0.101	0.065	1.55	4500	262	0.097	0.065	1.49	4640	263	0.096	0.065	1.48	4690
	275	.109	.061	1.79	4645	281	.109	.061	1.79	4750	278	.105	.061	1.72	4810
	292	.118	.061	1.93	4685	296	.117	.060	1.95	4800	308	.122	.061	2.00	4830
	309	.133	.060	2.22	4600	315	.126	.057	2.21	4940	332	.036	.061	2.23	4840
	309	.141	.056	2.52	4500	320	.139	.056	2.48	4710	330	.138	.055	2.51	4910
	305	.145	.051	2.84	4470	318	.144	.050	2.88	4710	324	.141	.050	2.82	4870
	300	.149	.046	3.24	4420	308	.146	.045	3.24	4630	314	.146	.044	3.32	4750
	294	.155	.040	3.88	4330	303	.152	.039	3.90	4560	305	.152	.038	4.00	4610
	L*, 50 in.					L*, 75 in.					L*, 100 in.				
1	261	0.096	0.064	1.50	4680	266	0.099	0.065	1.52	4660	259	0.099	0.066	1.50	4510
	283	.107	.062	1.73	4810	282	.108	.062	1.74	4760	295	.115	.064	1.80	4730
	313	.123	.062	2.00	4860	324	.128	.062	2.06	4900	314	.127	.061	2.08	4800
	328	.130	.059	2.20	4980	340	.137	.059	2.32	4980	323	.132	.059	2.24	4860
	322	.134	.055	2.46	4890	326	.135	.053	2.55	4980	336	.141	.054	2.61	4950
	329	.141	.050	2.85	4970	335	.142	.049	2.90	5040	330	.140	.049	2.86	5010
	318	.145	.044	3.30	4830	324	.146	.043	3.40	4920	323	.145	.043	3.37	4930
	324	.150	.043	3.49	4820	316	.153	.038	4.03	4750	314	.153	.037	4.14	4750
2						282	.105	.062	1.69	4710	284	.108	.064	1.69	4600
						321	.122	.062	1.97	4860	299	.117	.060	1.95	4710
						298	.115	.055	2.09	4885	321	.126	.059	2.14	4835
						323	.126	.054	2.33	5000	327	.130	.057	2.28	4870
						339	.138	.052	2.65	4970	339	.139	.052	2.67	4945
						332	.141	.046	3.07	4950	329	.140	.046	3.04	4930
						316	.148	.038	3.89	4730	314	.150	.038	3.95	4655
						318	.166	.035	4.74	4410	316	.163	.035	4.66	4450
	Allylamine; A_t = [c]0.0905, [d]0.0864, and [e]0.0872 sq in.														
	L*, 20 in.					L*, 30 in.					L*, 40 in.				
1	365	0.165	0.085	1.94	4250	373	0.164	0.087	1.90	4330	379	0.163	0.084	1.95	4480
	359	.171	.078	2.21	4210	369	.170	.076	2.24	4370	372	.166	.075	2.21	4500
	349	.175	.069	2.55	4175	358	.175	.068	2.60	4300	364	.171	.067	2.55	4460
	307	.190	.056	3.42	3640	347	.183	.060	3.07	4180	358	.178	.058	3.07	4420
	295	.193	.054	3.57	3480	320	.192	.053	3.62	3805	333	.186	.052	3.61	4090
	275	.200	.049	4.08	3220	309	.193	.050	3.86	3700	321	.188	.049	3.88	3955
						287	.200	.046	4.35	3600	300	.198	.044	4.50	3610
	L*, 50 in.					L*, 75 in.					L*, 100 in.				
2	397	0.161	0.083	1.95	4535	394	0.159	0.078	2.05	4630	402	0.160	0.081	1.98	4640
	387	.158	.072	2.19	4675	391	.160	.070	2.29	4730	396	.160	.073	2.21	4740
	378	.165	.063	2.62	4610	385	.165	.060	2.75	4750	387	.162	.060	2.70	4850
	366	.172	.053	3.24	4520	378	.169	.053	3.21	4750	378	.168	.049	3.43	4850
	348	.184	.048	3.87	4180	362	.181	.045	4.02	4460	368	.180	.042	4.30	4600
	334	.192	.042	4.57	3970	344	.189	.040	4.73	4180	356	.182	.040	4.61	4510
	319	.196	.039	5.03	3770	339	.184	.038	4.84	4250	340	.188	.036	5.22	4255
3	374	.167	.063	2.63	4560										
	383	.179	.058	3.07	4530										
	366	.187	.049	3.80	4350										
	317	.195	.040	4.86	3790										

[a]First series of runs for UDMH.

[b]Second series of runs for UDMH.

[c]First series of runs for allylamine.

[d]Second series of runs for allylamine.

[e]Third series of runs for allylamine.

TABLE II. - Continued. BASIC EXPERIMENTAL DATA

[1-in. diam. chamber used except where noted]

Chamber pressure, p_c, lb/sq in. abs	Acid flow, w_o, lb/sec	Fuel flow, w_f, lb/sec	Acid-fuel weight ratio, o/f	Characteristic exhaust velocity, c*, ft/sec
o-Toludine; A_t = 0.0920 sq in.				
L*, 30 in.				
337	0.162	0.093	1.75	3920
336	.166	.083	2.00	4000
330	.171	.072	2.39	4030
324	.176	.062	2.83	4040
311	.182	.053	3.43	3920
311	.196	.052	3.77	3720
304	.203	.047	4.32	3600
L*, 75 in.				
356	0.157	0.088	1.78	4310
319	.139	.090	1.54	4130
339	.155	.074	2.09	4390
349	.171	.059	2.90	4500
340	.176	.049	3.63	4480
344	.187	.044	4.25	4410
343	.205	.038	5.39	4180
L*, 40 in.				
350	0.159	0.091	1.74	4160
345	.164	.080	2.05	4190
334	.167	.072	2.32	4140
333	.174	.062	2.82	4175
316	.180	.053	3.43	4030
314	.190	.049	3.88	3890
313	.206	.046	4.48	3680
L*, 100 in.				
354	0.158	0.088	1.80	[a]4265
364	.163	.079	2.06	4460
349	.163	.066	2.47	[a]4520
360	.169	.057	2.96	4720
346	.175	.046	3.80	4640
358	.188	.044	4.27	4570
345	.211	.033	6.39	4190
L*, 50 in.				
350	0.155	0.086	1.80	4300
357	.160	.078	2.05	4440
345	.167	.069	2.42	4330
312	.177	.049	3.61	4090
300	.211	.039	5.41	3550
348	.157	.091	1.73	4160
345	.162	.080	2.03	4225
342	.167	.071	2.35	4260
331	.172	.060	2.87	4230
324	.177	.052	3.40	4190
324	.190	.047	4.04	4050
317	.209	.044	4.75	3710
Hydrazine; 1.5-in.-diam. chambers; A_t = 0.0848 sq in.				
L*, 33 in.				
245	0.062	0.076	0.82	4860
240	.066	.070	.94	4810
239	.074	.062	1.19	4810
257	.081	.065	1.25	4810
260	.092	.061	1.50	4630
276	.104	.061	1.71	4565
269	.113	.057	1.98	4340
282	.127	.055	2.28	4225
L*, 100 in.				
241	0.063	0.076	0.83	4750
231	.062	.070	.90	4770
231	.067	.065	1.01	4780
250	.077	.062	1.25	4910
279	.091	.062	1.48	4980
317	.119	.064	1.86	4720
286	.120	.057	2.11	4410
285	.130	.055	2.36	4210
L*, 50 in.				
234	0.058	0.075	0.77	4780
253	.068	.070	.96	5010
250	.068	.066	1.03	5060
261	.079	.062	1.27	5050
274	.092	.061	1.50	4860
284	.102	.061	1.68	4770
300	.121	.060	2.02	4520
297	.130	.057	2.27	4325
L*, 144 in.				
230	0.060	0.074	0.80	4710
229	.065	.069	.94	4680
232	.069	.065	1.06	4700
264	.084	.065	1.30	4860
273	.092	.062	1.50	4850
300	.110	.063	1.75	4760
274	.114	.056	2.05	4410
290	.126	.057	2.21	4320
L*, 75 in.				
225	0.058	0.075	0.77	4630
241	.065	.070	.92	4890
247	.069	.067	1.03	4940
270	.083	.064	1.31	5015
306	.101	.066	1.52	5000
312	.113	.064	1.77	4830
316	.125	.061	2.04	4620
306	.132	.057	2.31	4400
Hydrazine; 2-in.-diam. chambers; A_t = 0.0848 sq in.				
L*, 50 in.				
238	0.064	0.074	0.86	4700
233	.067	.069	.97	4680
234	.068	.065	1.05	4810
257	.088	.064	1.38	4615
269	.103	.062	1.66	4440
272	.109	.060	1.82	4390
291	.128	.060	2.13	4220
285	.132	.056	2.36	4140
L*, 171 in.				
242	0.064	0.076	0.83	4715
241	.065	.071	.91	4835
256	.073	.069	1.06	4920
252	.078	.064	1.21	4825
269	.092	.060	1.53	4810
313	.113	.065	1.73	4800
288	.118	.060	1.97	4430
288	.124	.057	2.17	4330
L*, 75 in.				
237	0.060	0.074	0.82	4820
236	.062	.071	.87	4840
255	.072	.068	1.06	4950
273	.085	.066	1.29	4900
262	.087	.061	1.42	4820
263	.093	.061	1.54	4695
299	.117	.061	1.92	4570
295	.126	.057	2.20	4390
L*, 300 in.				
244	0.066	0.077	0.85	4640
242	.067	.073	.92	4715
251	.073	.068	1.07	4840
276	.089	.066	1.35	4860
286	.096	.064	1.50	4880
278	.105	.059	1.80	4630
297	.118	.061	1.92	4540
284	.126	.056	2.25	4250
L*, 100 in.				
255	0.066	0.076	0.87	4920
244	.065	.072	.90	4880
261	.074	.069	1.08	4960
270	.081	.067	1.22	4970
296	.098	.066	1.50	4940
308	.109	.065	1.69	4850
289	.110	.059	1.84	4660
297	.120	.058	2.09	4560

[a]Audible scream.

TABLE II. - Concluded. BASIC EXPERIMENTAL DATA

[1-in. diam. chamber used except where noted]

Chamber pressure, p_c, lb/sq in. abs	Acid flow, w_o, lb/sec	Fuel flow, w_f, lb/sec	Acid-fuel weight ratio, o/f	Characteristic exhaust velocity c*, ft/sec
Unsymmetrical dimethylhydrazine; 1.5-in.-diam. chambers; A_t = 0.0850 sq in.				
L*, 33 in.				
262	0.094	0.066	1.42	4480
283	.107	.062	1.73	4580
297	.117	.061	1.92	4570
330	.136	.061	2.23	4580
326	.138	.056	2.46	4600
324	.142	.051	2.78	4590
314	.146	.046	3.17	4480
308	.153	.039	3.92	4390
L*, 50 in.				
269	0.095	0.064	1.48	4630
286	.103	.062	1.66	4740
308	.114	.060	1.90	4840
331	.127	.059	2.15	4870
337	.134	.055	2.44	4880
332	.138	.050	2.76	4830
325	.142	.045	3.16	4760
315	.150	.037	4.05	4610
235	.081	.068	1.19	4320
261	.091	.065	1.40	4580
279	.099	.063	1.57	4710
311	.115	.061	1.89	4840
337	.135	.055	2.46	4855
333	.139	.050	2.78	4820
325	.144	.044	3.27	4730
316	.153	.038	4.03	4530
L*, 75 in.				
274	0.094	0.066	1.43	4690
301	.107	.062	1.73	4880
333	.123	.062	1.98	4930
359	.136	.060	2.26	5010
349	.134	.055	2.44	5050
342	.138	.049	2.82	5010
333	.141	.043	3.28	4950
323	.150	.037	4.06	4730
L*, 100 in.				
270	0.096	0.065	1.48	4590
311	.112	.064	1.75	4840
316	.116	.060	1.93	4910
329	.123	.058	2.12	4975
347	.133	.055	2.42	5050
345	.138	.049	2.82	5050
336	.143	.043	3.32	4940
325	.151	.037	4.08	4730
L*, 144 in.				
270	0.096	0.066	1.45	4560
294	.107	.063	1.70	4730
314	.117	.061	1.92	4830
336	.128	.060	2.13	4890
345	.133	.055	2.42	5020
343	.136	.049	2.78	5075
334	.141	.043	3.28	4970
325	.149	.037	4.03	4780
Unsymmetrical dimethylhydrazine; 2-in.-diam. chambers; A_t = 0.0850 sq in.				
L*, 50 in.				
257	0.097	0.067	1.45	4290
280	.109	.064	1.70	4430
309	.126	.063	2.00	4475
329	.136	.063	2.16	4525
322	.139	.056	2.48	4520
316	.141	.051	2.76	4505
307	.145	.046	3.15	4400
303	.152	.040	3.80	4320
L*, 75 in.				
261	0.091	0.065	1.40	4580
294	.107	.062	1.73	4760
312	.117	.061	1.92	4800
329	.126	.059	2.14	4870
340	.135	.055	2.45	4900
338	.137	.050	2.74	4950
328	.141	.044	3.20	4850
315	.150	.038	3.95	4590
L*, 100 in.				
265	0.090	0.064	1.41	4710
296	.105	.061	1.72	4880
326	.119	.060	1.98	4980
359	.134	.060	2.23	5060
342	.130	.053	2.45	5115
348	.138	.048	2.88	5120
340	.143	.041	3.49	5060
328	.152	.036	4.22	4775
L*, 171 in.				
268	0.097	0.064	1.52	4430
280	.104	.062	1.68	4620
322	.119	.062	1.92	4870
347	.131	.060	2.18	4970
351	.135	.054	2.50	5080
345	.139	.048	2.90	5050
337	.142	.043	3.30	4985
324	.152	.037	4.11	4690
L*, 300 in.				
259	0.097	0.065	1.49	4375
287	.110	.062	1.77	4570
305	.119	.060	1.98	4660
349	.136	.061	2.23	4845
344	.136	.054	2.52	4955
341	.140	.049	2.86	4940
332	.144	.043	3.35	4860
318	.152	.037	4.11	4605

TABLE III. - FUEL RATINGS; CHARACTERISTIC LENGTH L^*_{97} AS FUNCTION OF β

Fuel	Stoichiometric o/f ratio	L^*_{97} for β of -				
		0.55	0.65	0.80	1.00	1.25
Hydrazine	1.48	----	16.0	19.0	19.5	19.5
TMTP	2.80	----	24.0	27.5	21.5	25.0
Furfuryl alcohol	2.85	----	25.0	31.0	40.0	48.0
UDMH	3.38	24.5	28.5	37.0	42.5	----
Allylamine[a]	4.23	54.0	60.0	75.0	84.0	----
o-Toluidine[a]	4.38	75.0	80.0	83.0	76.0	----

[a]Minimum values based on c^* at an L^* of 100 in.

TABLE IV. - MAXIMUM EXPERIMENTAL VALUES FOR CHARACTERISTIC EXHAUST VELOCITY c^*

Fuel	c^* for β of -				
	0.55	0.65	0.80	1.00	1.25
Hydrazine	----	4900	5010	4940	4720
TMTP	----	4050	4190	4160	3990
Furfuryl alcohol	----	4530	4600	4570	4400
UDMH	4870	4960	5010	4940	----
Allylamine[a]	4790	4860	4860	4650	----
o-Toluidine[a]	4590	4680	4700	4550	----

[a]Values at an L^* of 100 in.

TABLE V. - CHARACTERISTIC LENGTH L^*_{97} AS FUNCTION OF CHAMBER DIAMETER

Fuel	Diameter, in.	L^*_{97} for β of -		
		0.65	0.80	1.00
Hydrazine	1.0	16.0	19.0	19.5
	1.5	36.5	36.0	39.0
	2.0	50.0	56.5	76.0
UDMH	1.0	28.5	37.0	42.5
	1.5	49.5	56.0	60.0
	2.0	78.0	75.0	84.0

TABLE VI. - CORRELATION OF CHARACTERISTIC LENGTH L^*_{97} FOR VARIOUS CHAMBER DIAMETERS

Fuel	L^*_{97}(1.5-in. diam.) - L^*_{97}(1.0-in. diam.)			
	β			Average difference
	0.65	0.80	1.00	
Hydrazine	20.5	17.0	19.5	19.0
UDMH	21.0	19.0	17.5	19.2
	L^*_{97}(2-in. diam.) - L^*_{97}(1.0-in. diam.)			
Hydrazine	34.0	37.5	56.5	42.7
UDMH	49.5	38.0	41.5	43.0

TABLE VII. - COMPARISON OF CHARACTERISTIC LENGTH L^*_{97}, CUP PRESSURE DROP, AND IGNITION DELAY VALUES

Fuel	L^*_{97}[a], in.	Cup pressure drop[a], lb/sq in.	Ignition delay, millisec
Hydrazine	16	305	[b]6
TMTP	24	129	[c]7.6
Furfuryl alcohol	25	81	[d]25
UDMH	28.5	124	[e]2
Allylamine	[f]60	100	[d]310
o-Toluidine	[f]80	88	[d]350

[a]Taken at β of 0.65.
[b]With WFNA, 70° F, ref. 17.
[c]With RFNA (18 percent NO_2), -40° F, ref. 18.
[d]With WFNA, 70° F, ref. 19.
[e]With RFNA, -65° to 70° F, ref. 10.
[f]Minimum values based on c^* at an L^* of 100 in.

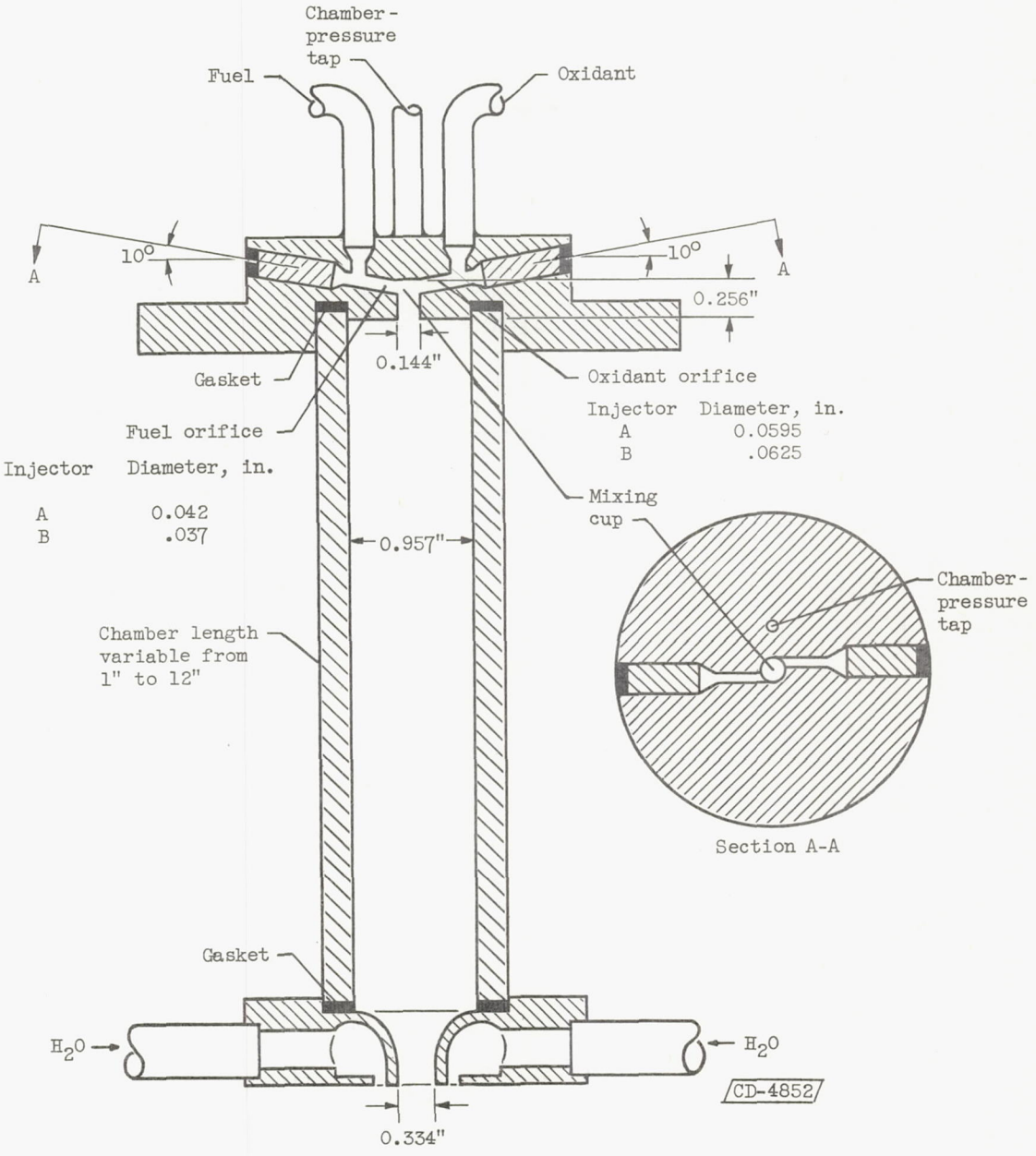

Figure 1. - Cross section of rocket-engine assembly.

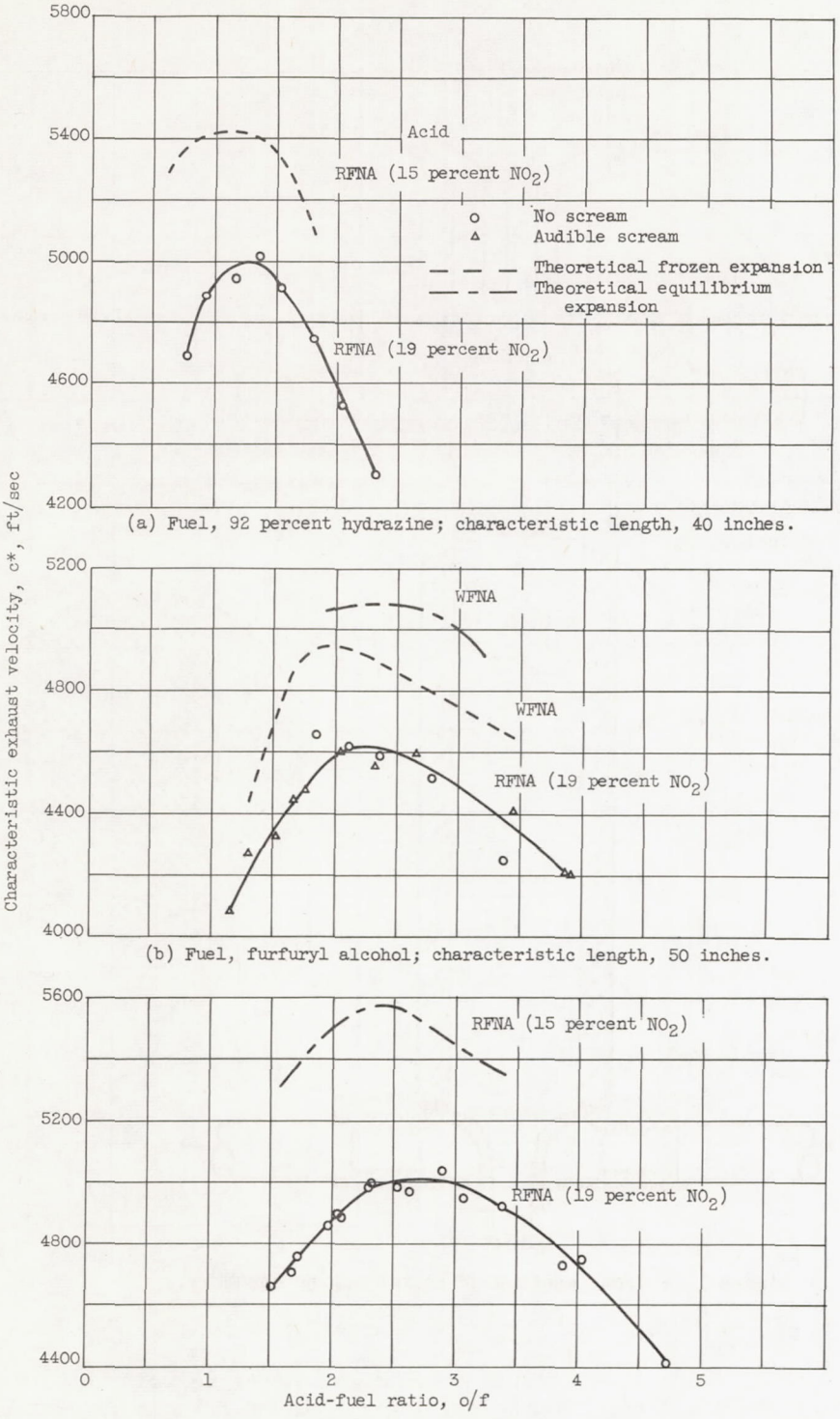

(a) Fuel, 92 percent hydrazine; characteristic length, 40 inches.

(b) Fuel, furfuryl alcohol; characteristic length, 50 inches.

(c) Fuel, UDMH; characteristic length, 75 inches.

Figure 2. - Characteristic exhaust velocity as function of acid-fuel ratio at characteristic length of maximum experimental characteristic exhaust velocity.

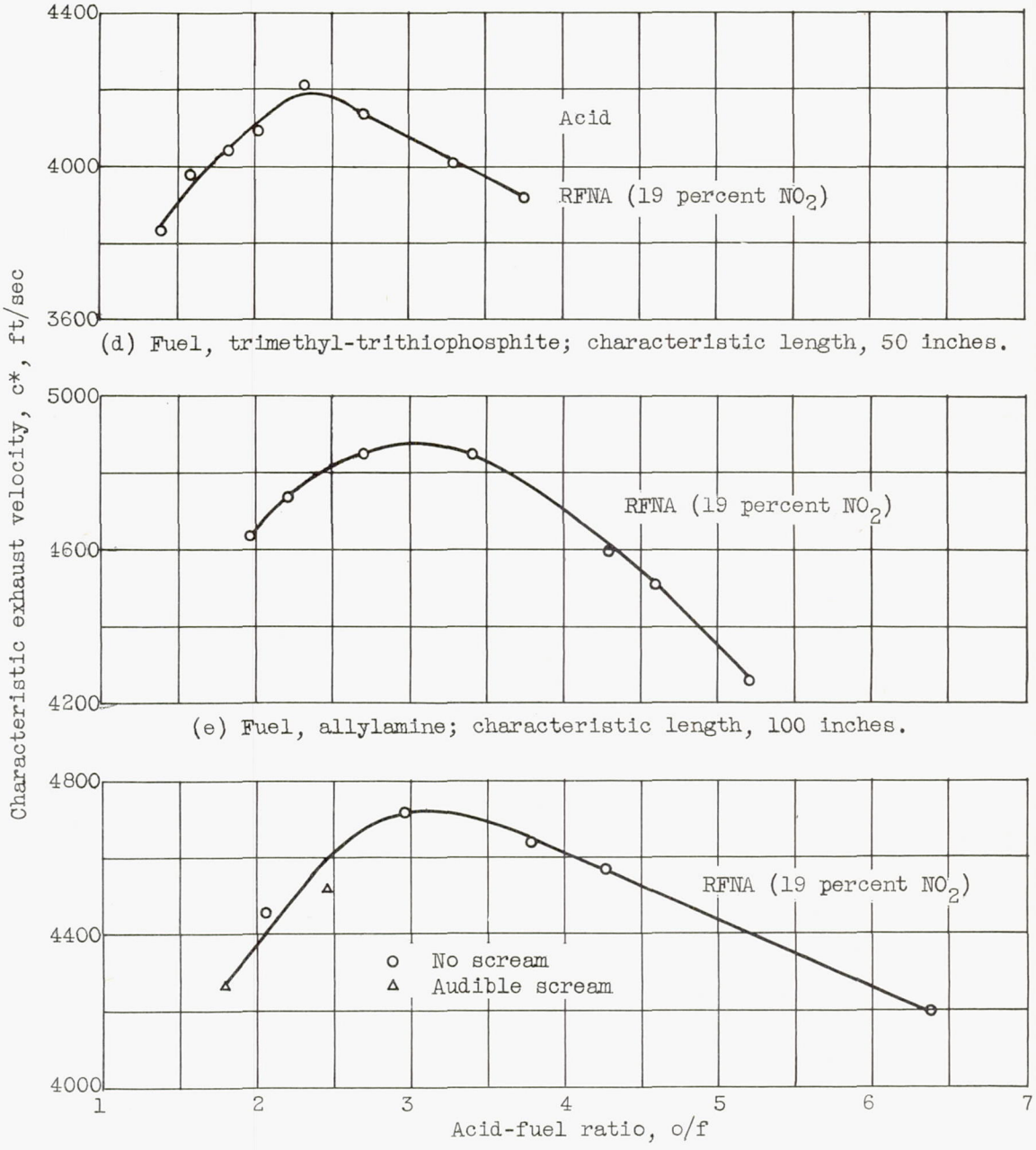

(d) Fuel, trimethyl-trithiophosphite; characteristic length, 50 inches.

(e) Fuel, allylamine; characteristic length, 100 inches.

(f) Fuel, o-toluidine; characteristic length, 100 inches.

Figure 2. - Concluded. Characteristic exhaust velocity as function of acid-fuel ratio at characteristic length of maximum experimental characteristic exhaust velocity.

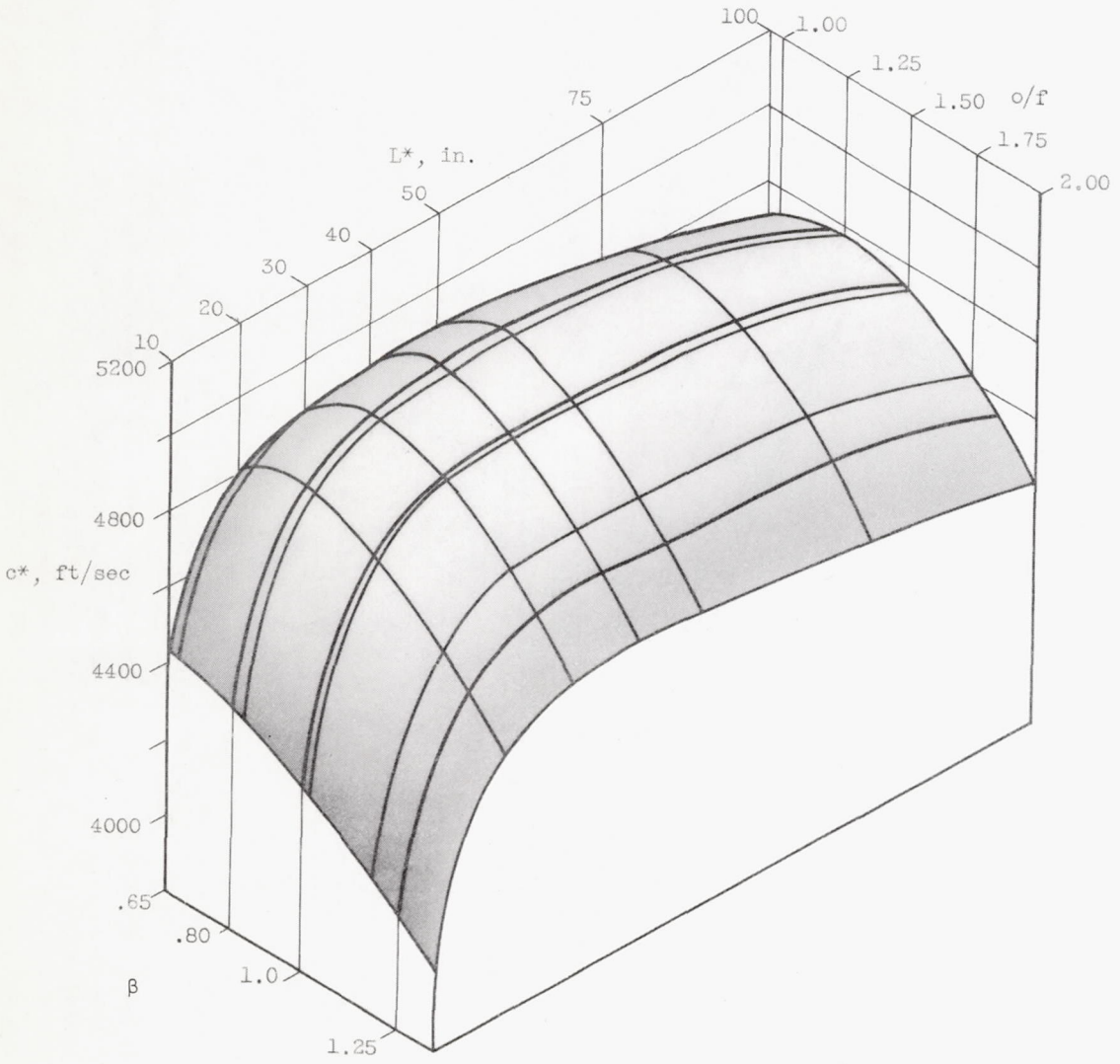

(a) Hydrazine.

Figure 3. - Characteristic exhaust velocity c* as function of characteristic length L* and acid-fuel ratio o/f in 1-inch-diameter chambers.

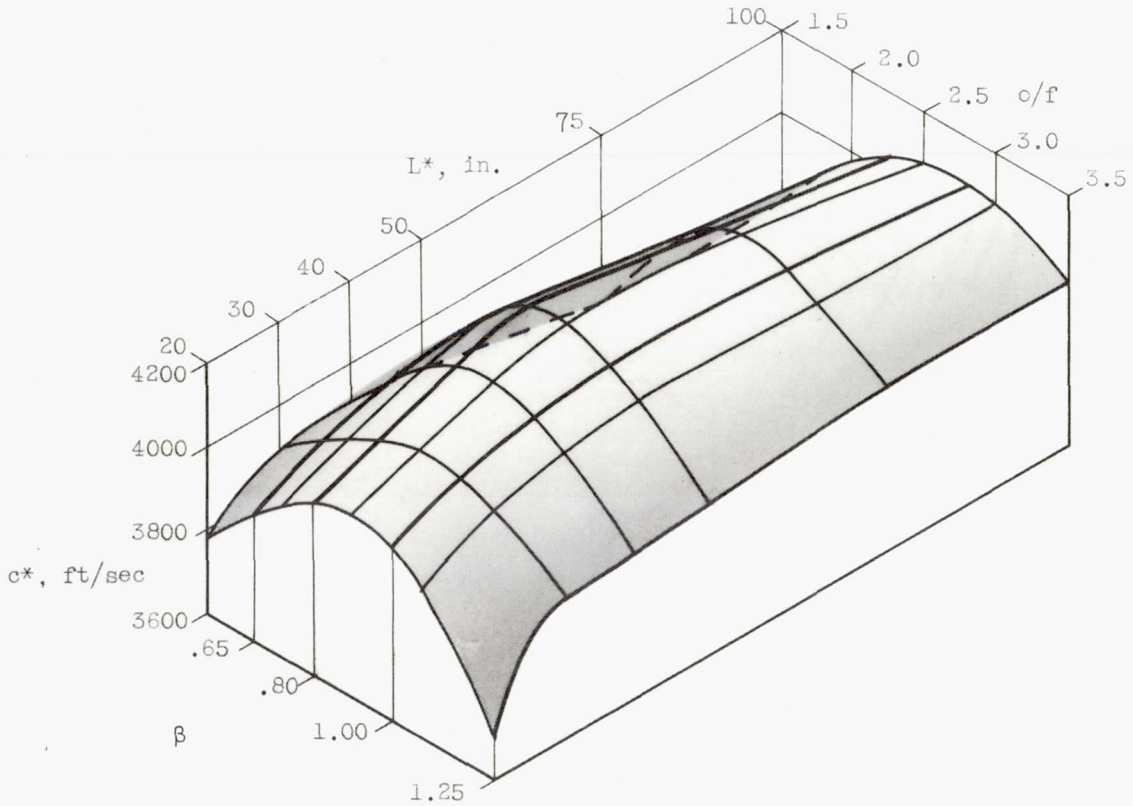

(b) Trimethyl-trithiophosphite.

Figure 3. - Continued. Characteristic exhaust velocity c* as function of characteristic length L* and acid-fuel ratio o/f in 1-inch-diameter chambers.

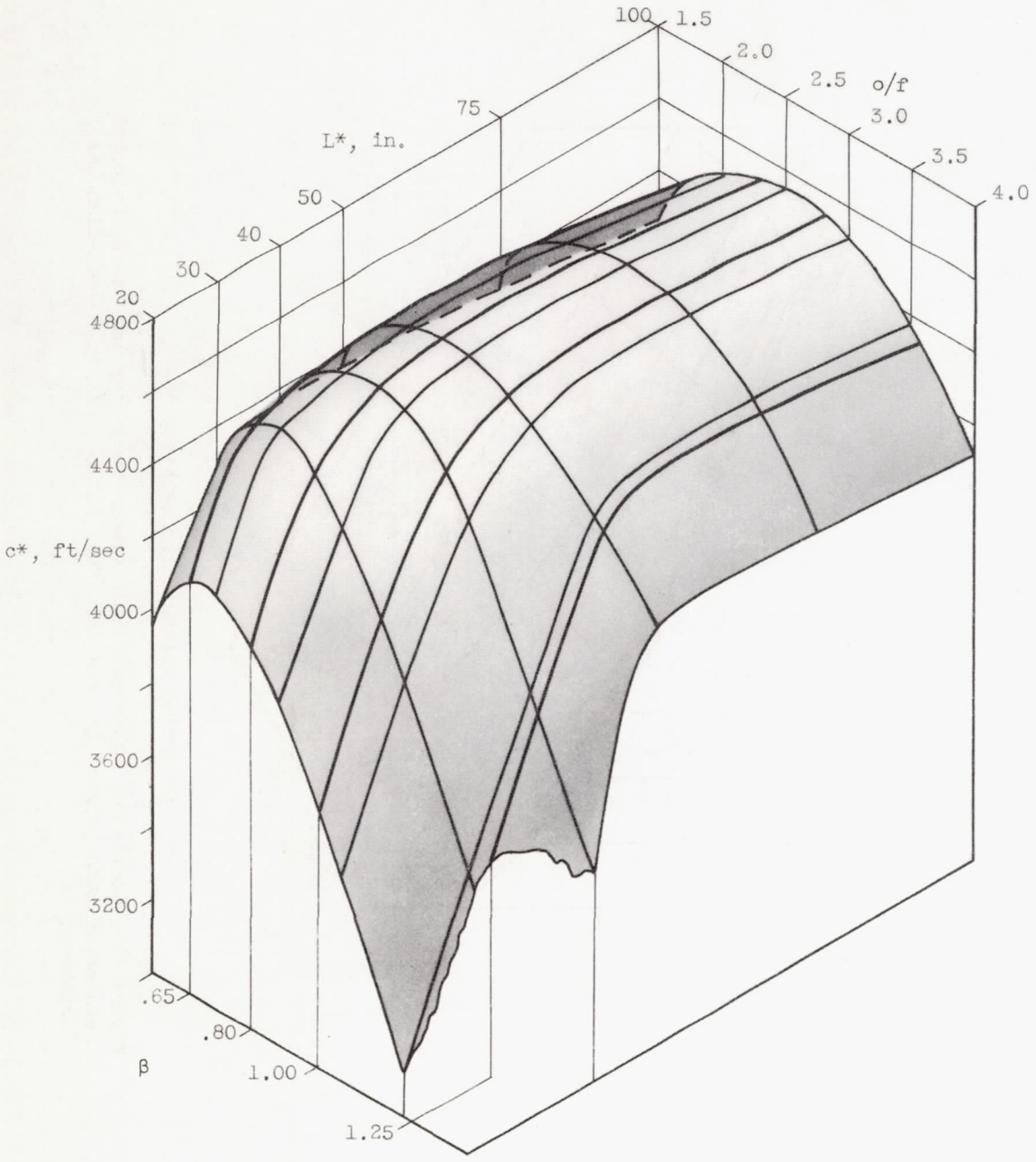

(c) Furfuryl alcohol.

Figure 3. - Continued. Characteristic exhaust velocity c* as function of characteristic length L* and acid-fuel ratio o/f in 1-inch-diameter chambers.

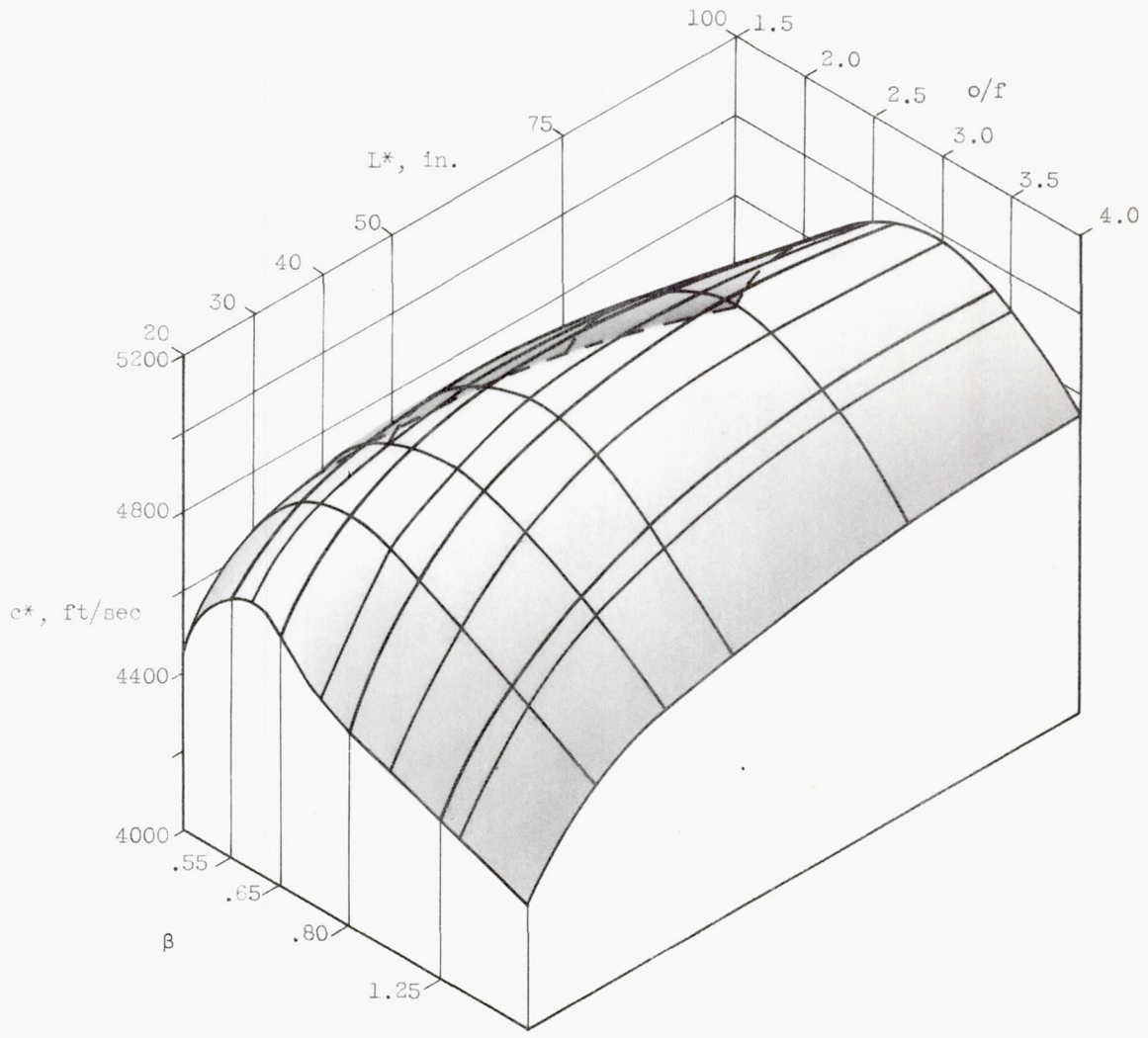

(d) Unsymmetrical dimethylhydrazine.

Figure 3. - Continued. Characteristic exhaust velocity c* as function of characteristic length L* and acid-fuel ratio o/f in 1-inch-diameter chambers.

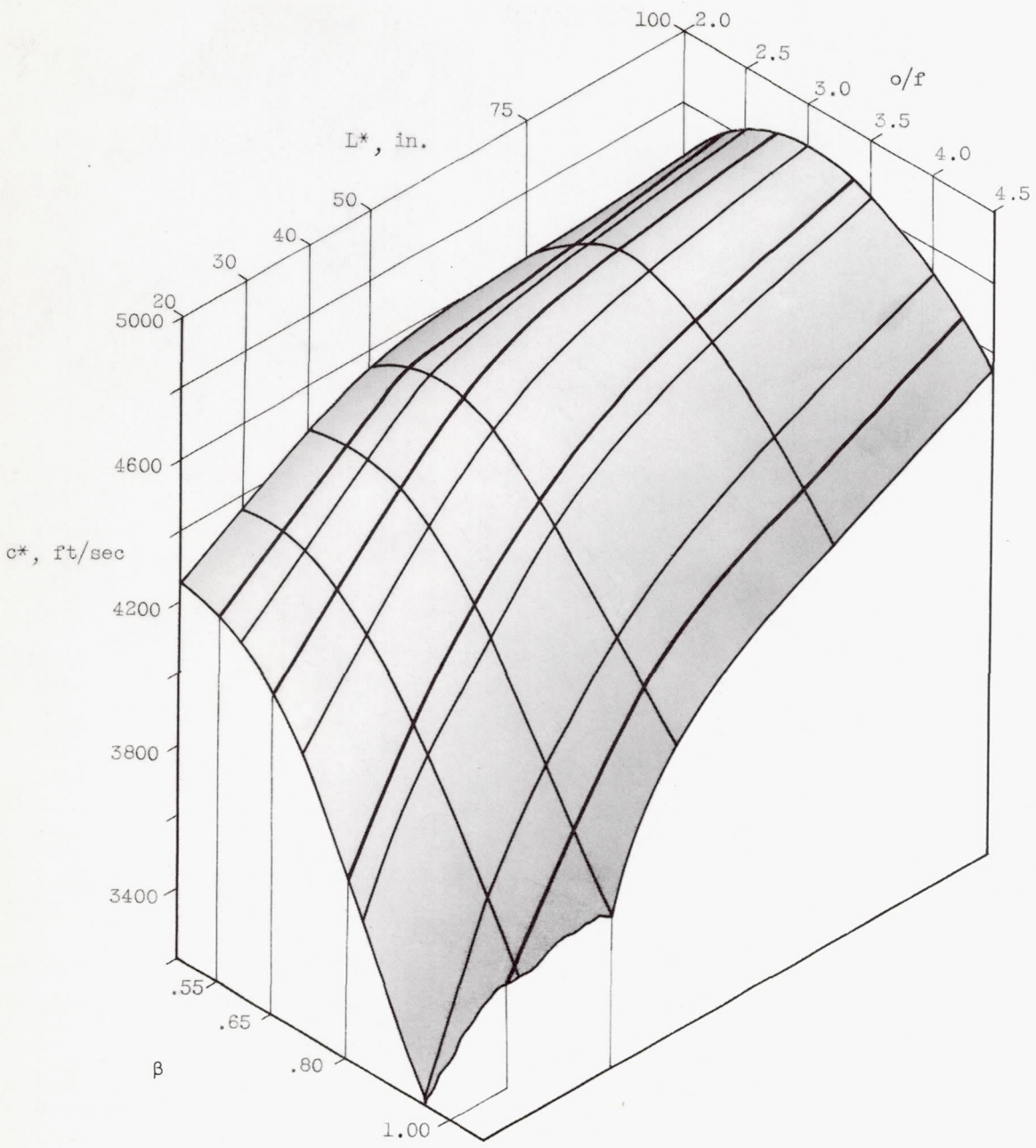

(e) Allylamine.

Figure 3. - Continued. Characteristic exhaust velocity c* as function of characteristic length L* and acid-fuel ratio o/f in 1-inch-diameter chambers.

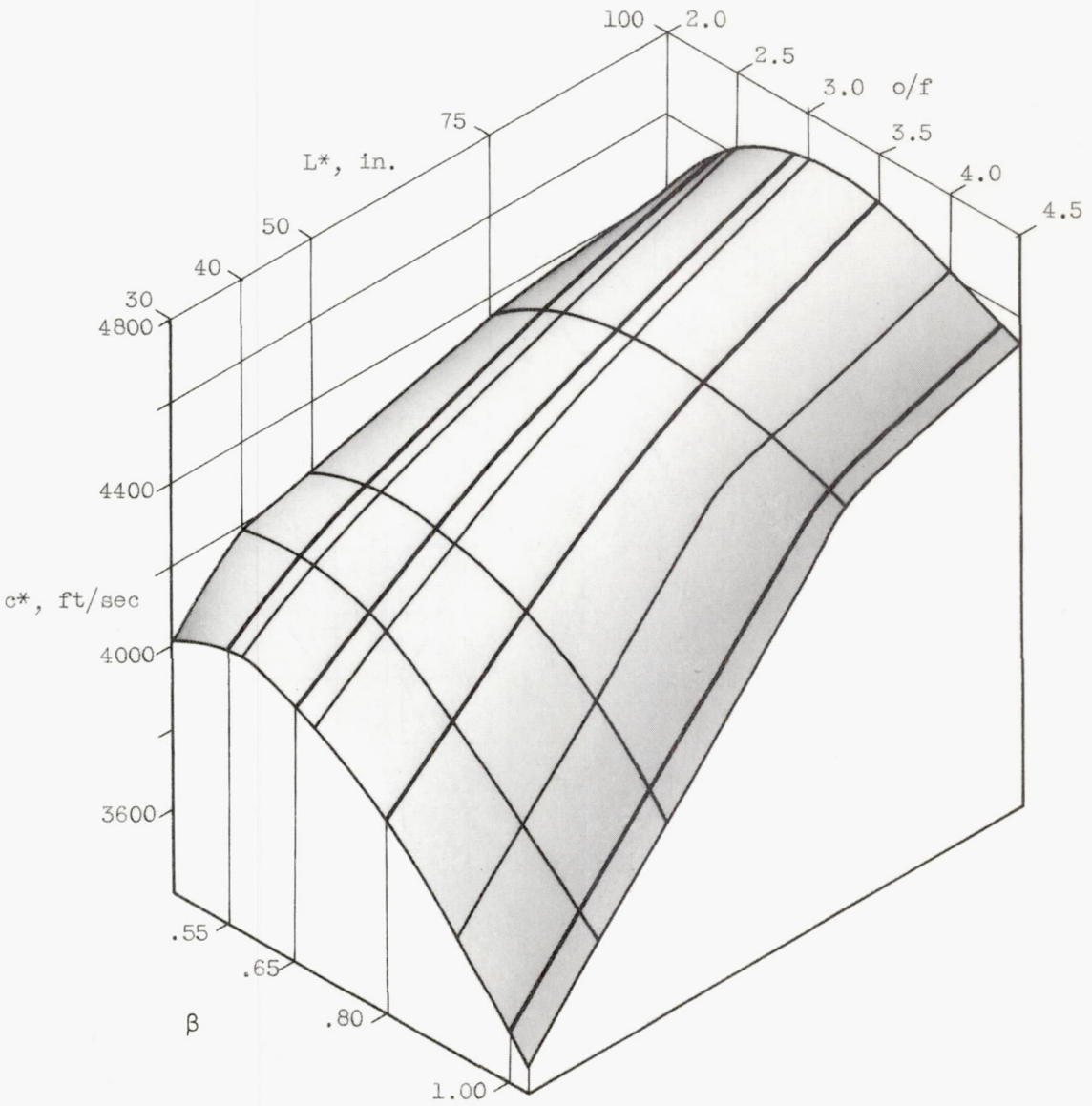

(f) o-Toluidine.

Figure 3. - Concluded. Characteristic exhaust velocity c* as function of characteristic length L* and acid-fuel ratio o/f in 1-inch-diameter chambers.

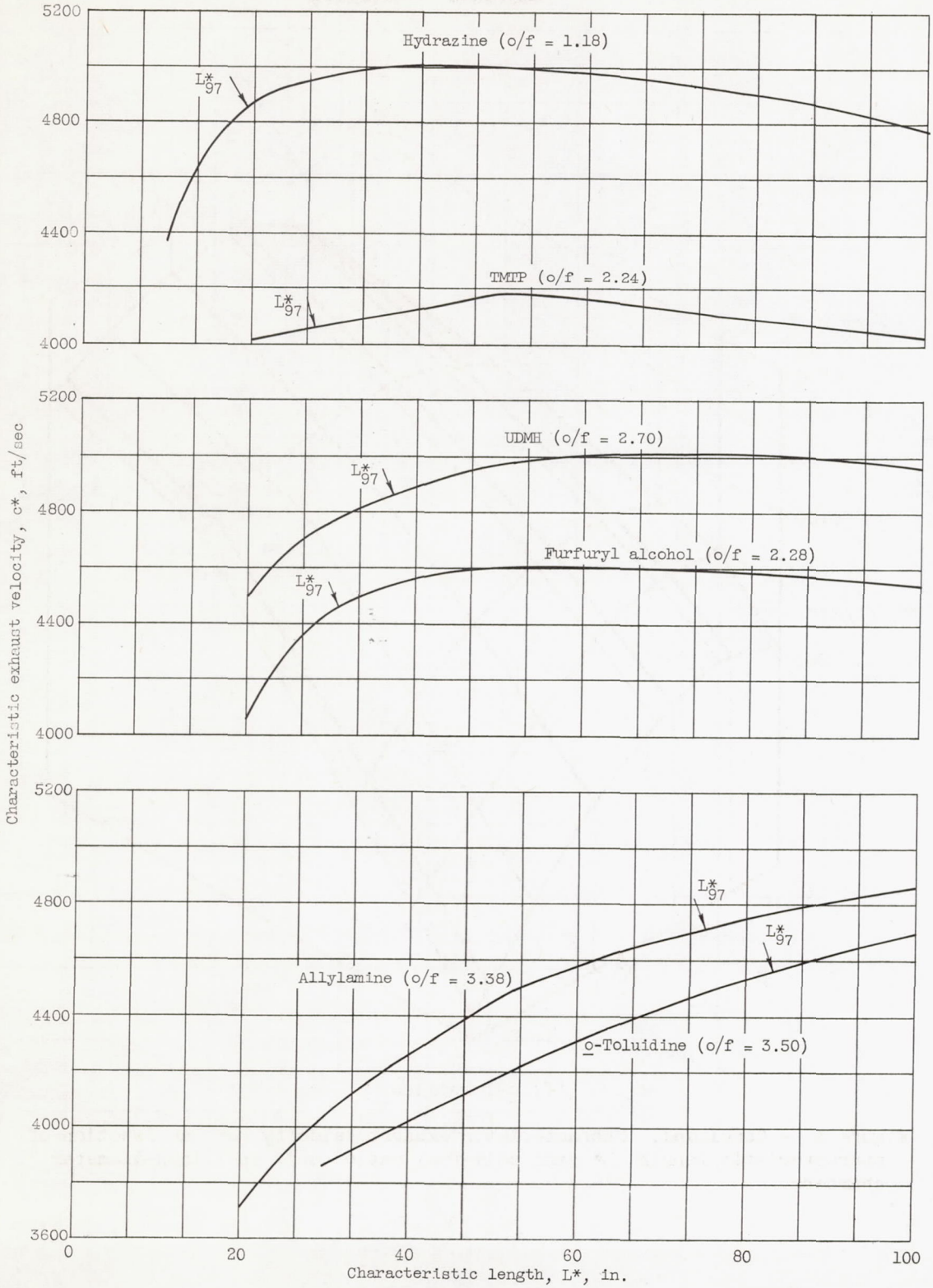

Figure 4. - Comparison of fuels at a β of 0.80.

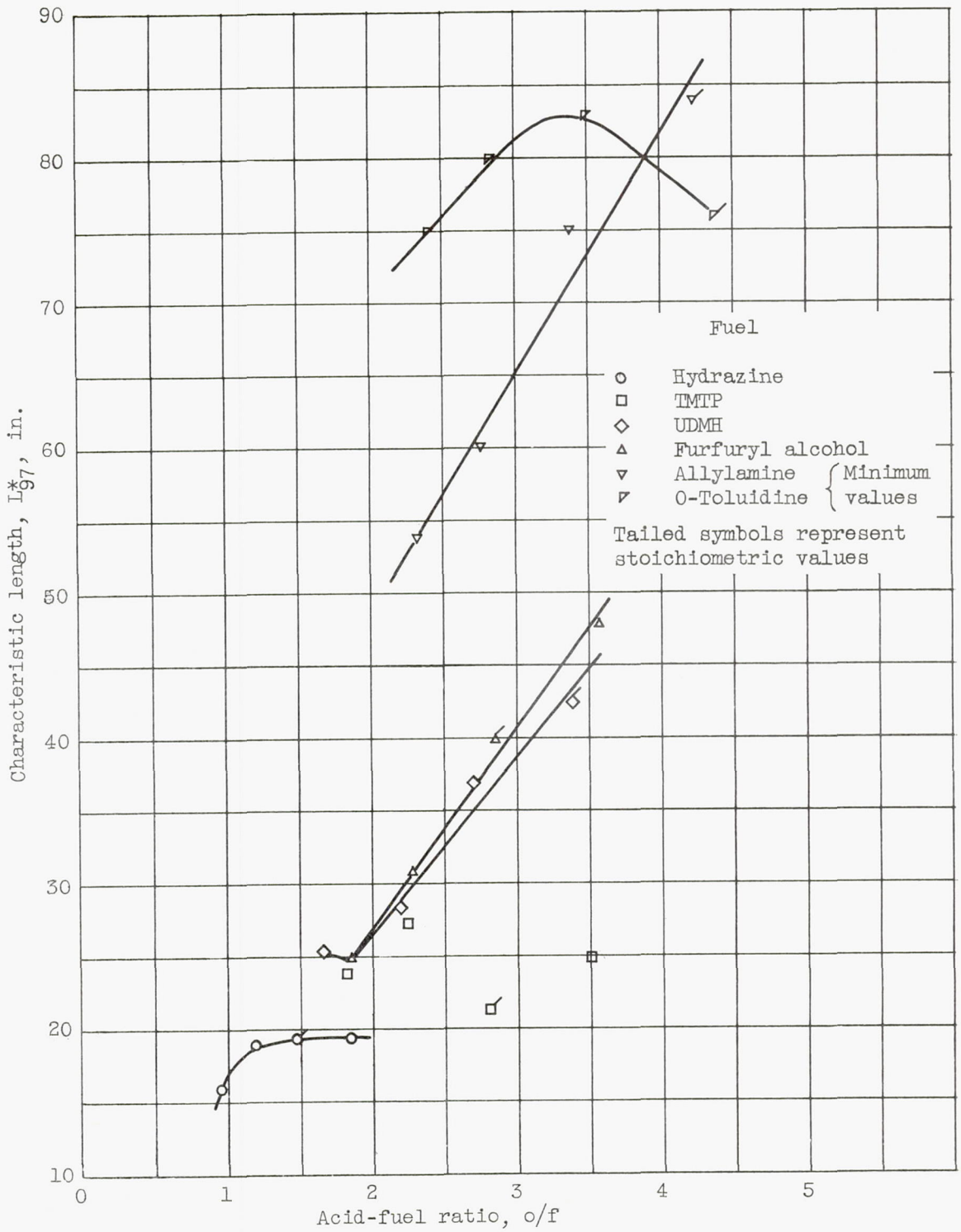

Figure 5. - Effect of stoichiometry; L^*_{97} as function of acid-fuel ratio.

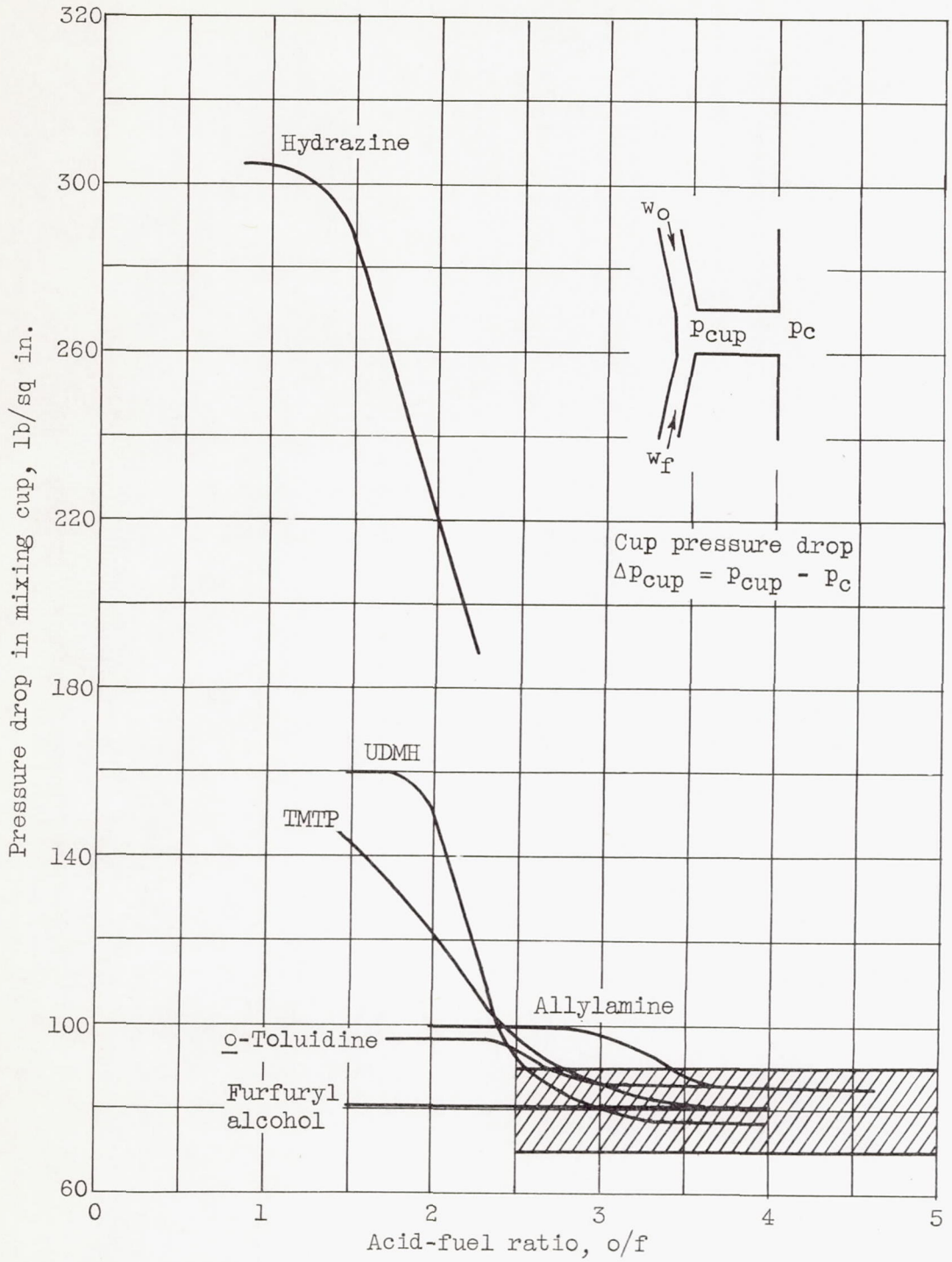

Figure 6. - Cup pressure drop reduced to uniform flow rate (w_T = 0.2 lb/sec) as function of acid-fuel ratio.

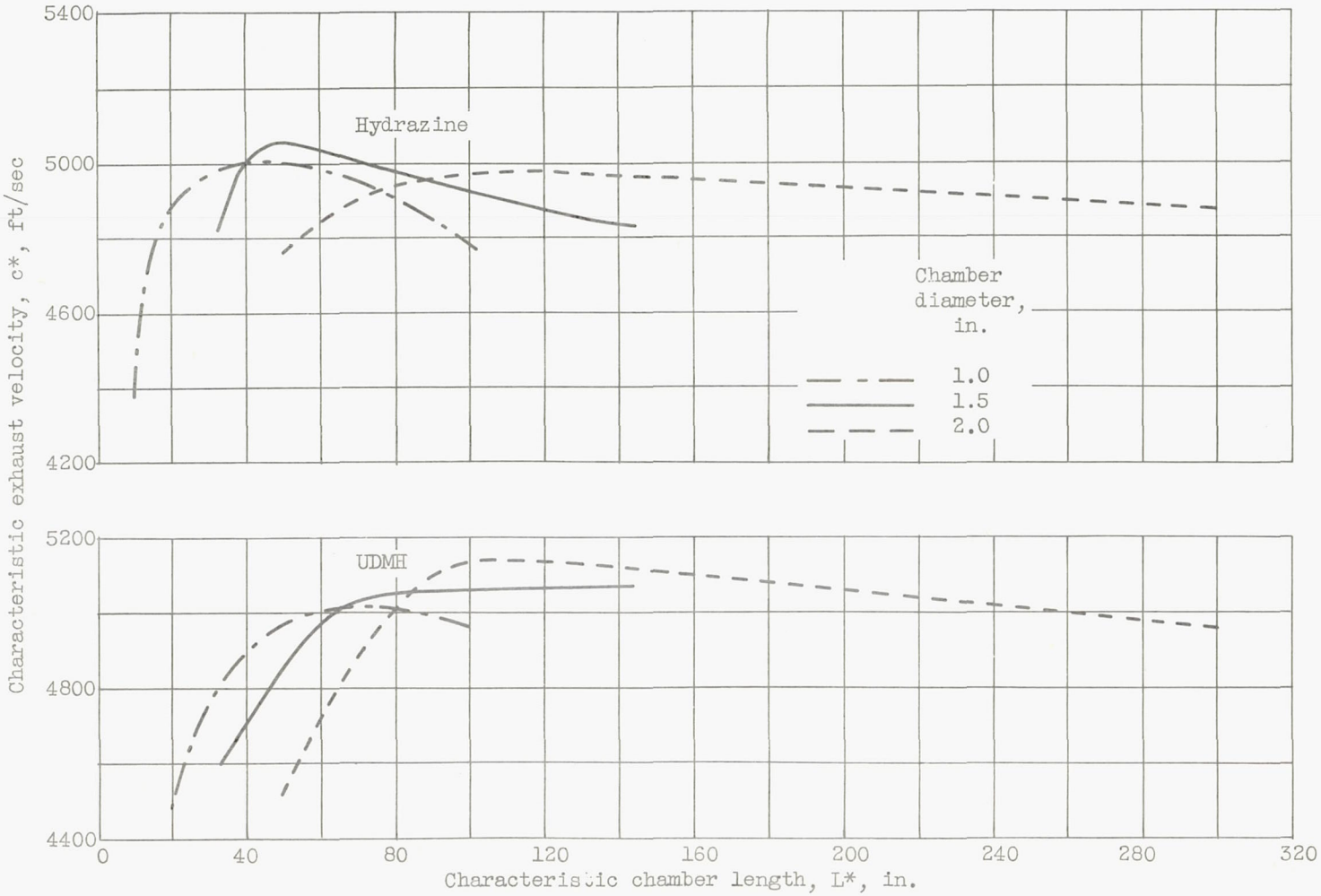

(a) As function of characteristic length.

Figure 7. - Effect of chamber diameter on characteristic exhaust velocity c* at a β of 0.80.

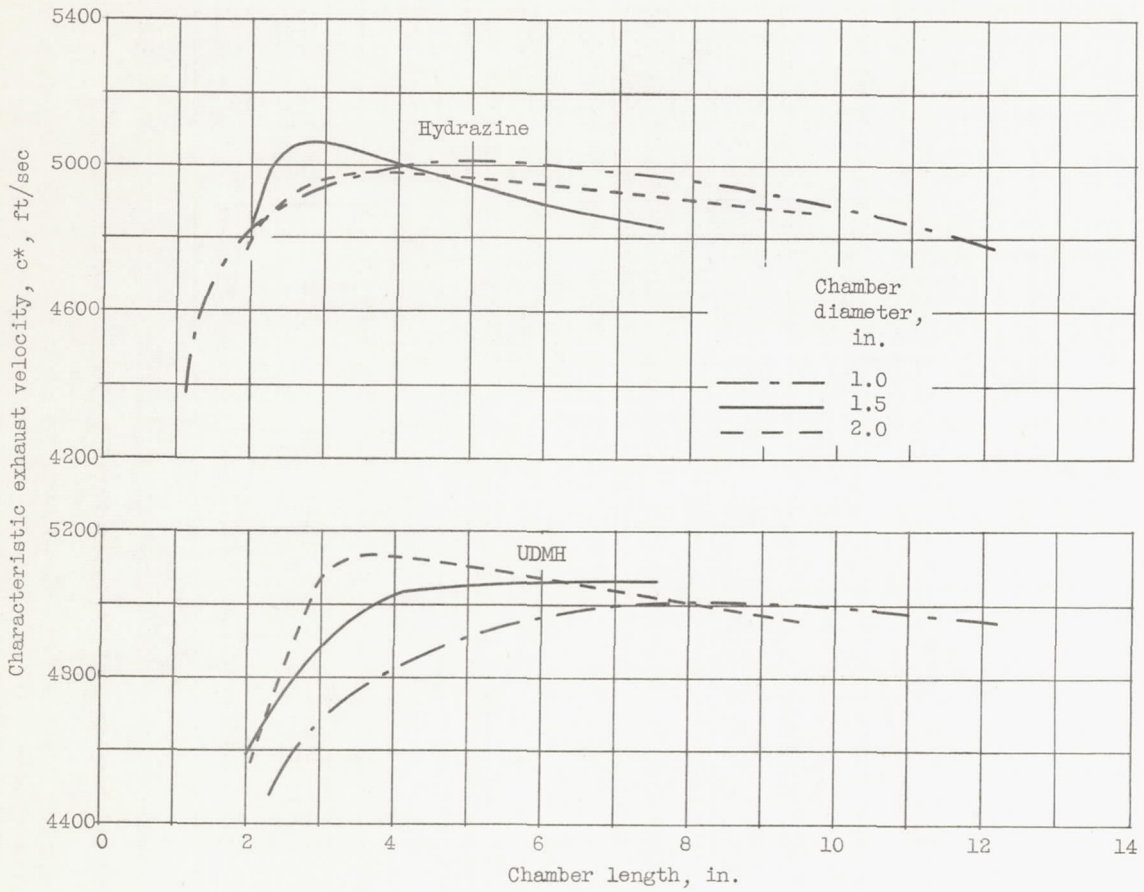

(b) As function of chamber length.

Figure 7. - Concluded. Effect of chamber diameter on characteristic exhaust velocity c* at a β of 0.80.

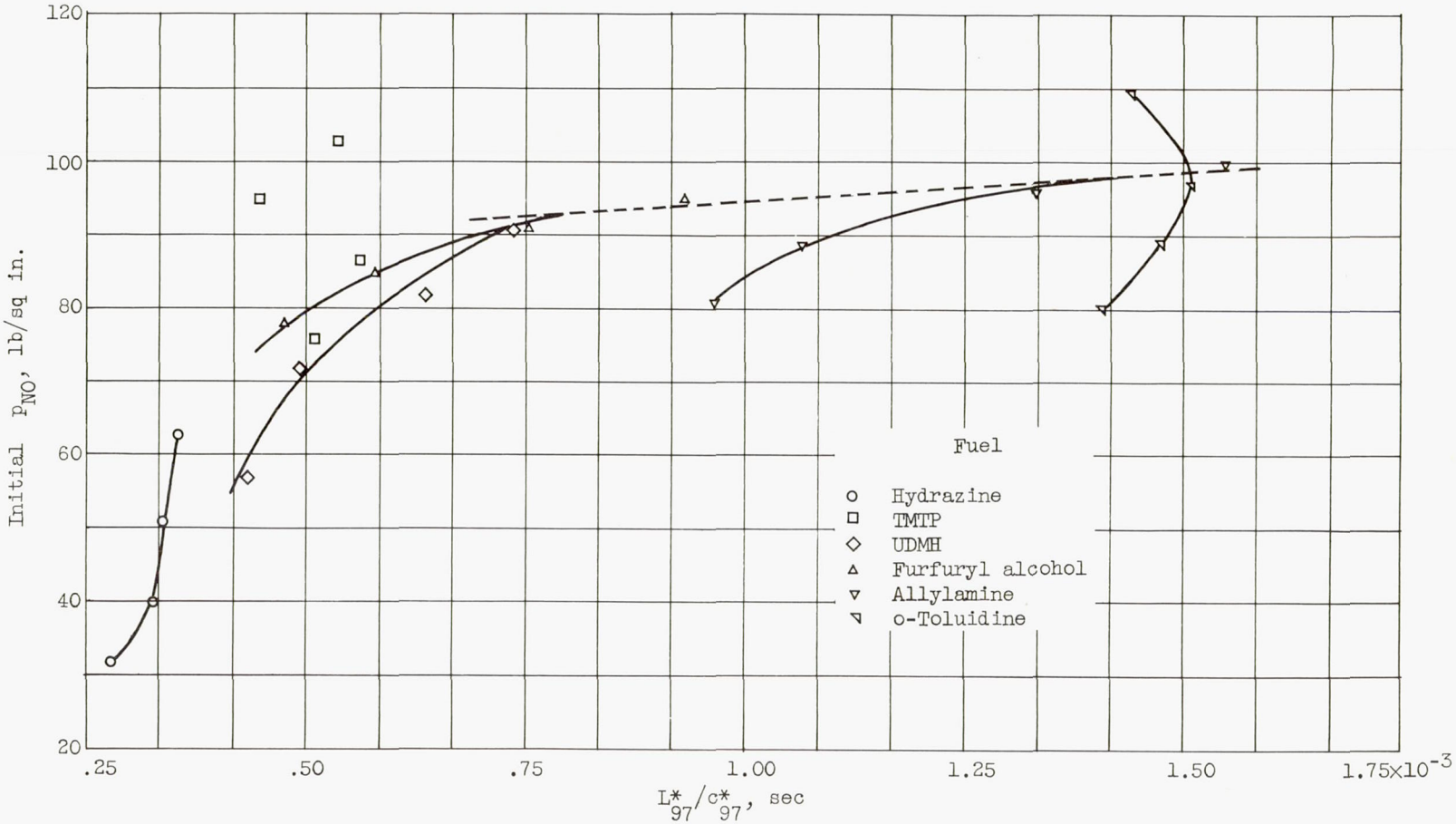

Figure 8. - Correlation of reactivity with initial NO concentration.

Figure 9. - Experimental apparatus for determining mixing efficiency of injectors.

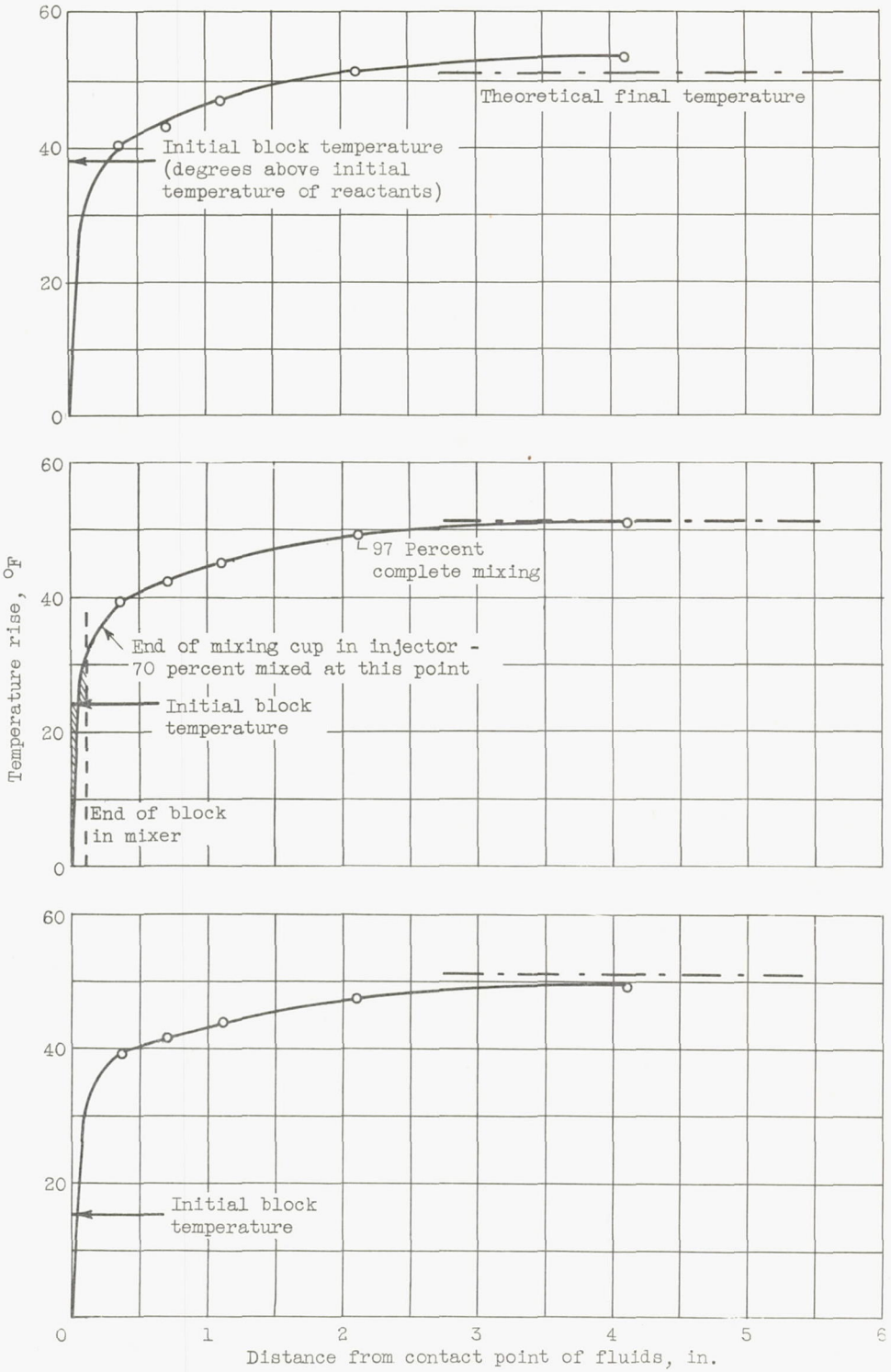

Figure 10. - Temperature rise as function of distance along mixer for three initial block temperatures.

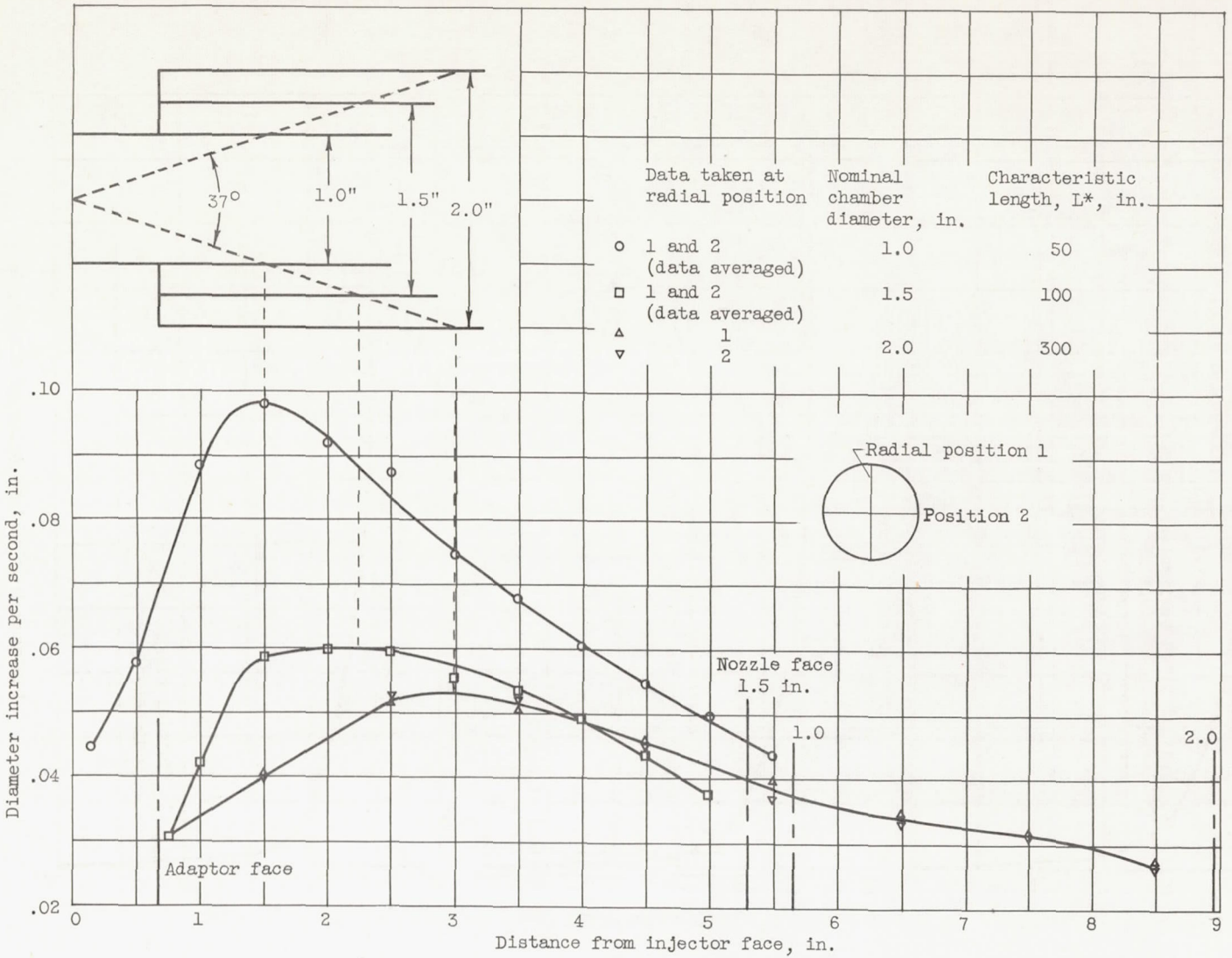

Figure 11. - Erosion pattern and its relation to diameter and chamber geometry. Fuel, hydrazine.

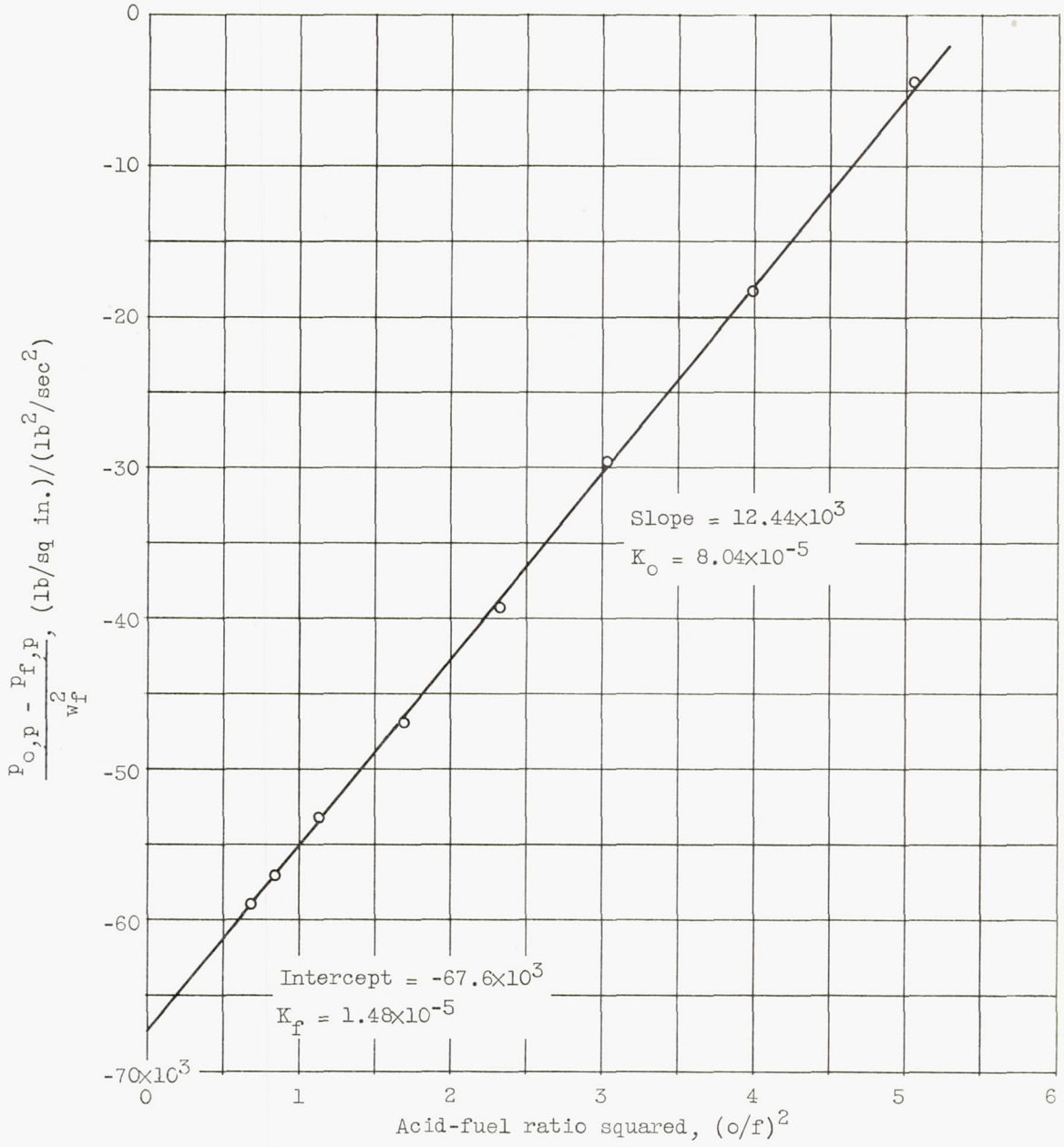

Figure 12. - Example of graphical calculation of flow constants K_o and K_f for hydrazine.